Journal Pre-proof

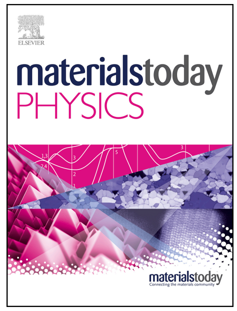

Flexible Discretely-Magnetized Configurable Soft Robots via Laser-tuned Selective Transfer Printing of Anisotropic Ferromagnetic Cells

Xingxing Ke, Shuo Zhang, Zhiping Chai, Jiajun Jiang, Yi Xu, Bo Tao, Han Ding, Zhigang Wu

PII: S2542-5293(20)30137-1

DOI: https://doi.org/10.1016/j.mtphys.2020.100313

Reference: MTPHYS 100313

To appear in: *Materials Today Physics*

Received Date: 7 October 2020

Revised Date: 1 November 2020

Accepted Date: 5 November 2020

Please cite this article as: X. Ke, S. Zhang, Z. Chai, J. Jiang, Y. Xu, B. Tao, H. Ding, Z. Wu, Flexible Discretely-Magnetized Configurable Soft Robots via Laser-tuned Selective Transfer Printing of Anisotropic Ferromagnetic Cells, *Materials Today Physics*, https://doi.org/10.1016/j.mtphys.2020.100313.

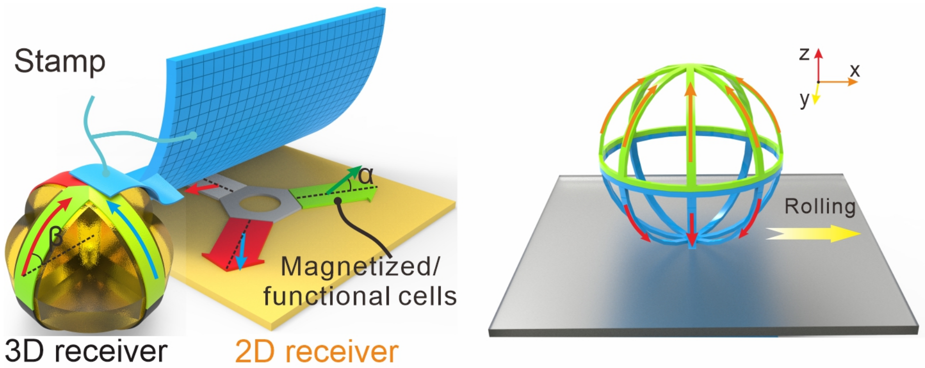
Stamp
Magnetized/
functional cells
3D receiver
2D receiver
β
α
z
x
y
Rolling

Flexible Discretely-Magnetized Configurable Soft Robots via Laser-tuned Selective Transfer Printing of Anisotropic Ferromagnetic Cells

Authors

Xingxing Ke [a], Shuo Zhang [a], Zhiping Chai [a], Jiajun Jiang [a], Yi Xu [a], Bo Tao [a], Han Ding [a,] **, Zhigang Wu [a,] *

Affiliations

[a] State Key Laboratory of Digital Manufacturing Equipment and Technology, School of Mechanical Science and Engineering, Huazhong University of Science and Technology, Wuhan 430074, China

* Corresponding author, ** Corresponding author.

Email: zgwu@hust.edu.cn (Z.W.); dinghan@hust.edu.cn (H.D.)

Abstract

Meso- or micro-scale soft robots with specific magnetization profiles have been demonstrated advanced locomotion capabilities in a plethora of unstructured environments. Despite some earlier success, technical challenges still exist for flexibly fabricating sophisticated constructed, heterogeneous and configurable soft magnetic robots at a relatively low cost. Here, by developing a new selective surface adhesion tuning, we report a transfer printing-based approach to flexibly configure magnetic domains for making 2/3-dimensional (2/3D) shaped fast-transforming untethered soft magnetic robots as well as heterogeneous integration of other desirable functional cells. This method enables physical realization of modular configurable magnetic robots integrated with specific magnetized profiles and other functional units like LEGO’s strategy. Further, we demonstrate a series of magnetic robots capable of configurable motion and responsive behaviors. This technique can serve as a new platform technique, potentially broadening the physical realization of heterogeneous integrable soft magnetic robots and empowering them with new capabilities and possibilities.

Keywords

Surface adhesion tuning, Selective transfer printing, Soft magnetic robots, Heterogeneous integration, Multifunctionalities

1. Introduction

More intimate interactions between robots and humans/environments are anticipated with the rapid advancement of robotic technologies [1], and further social interactions have been listed as one of the grand challenges of *Science Robotics*, recently [2]. Being able to attenuate external impacts and adapt their morphologies in complex environments naturally, soft robots demonstrate great advantages over rigid ones [3-8]. To maximally exploit the great potential of soft robots, an untethered realization or embodiment is desirable, although it is technically challenging [9]. Recently, new designs were reported by employing, e.g., hydrogen peroxide decomposition [10], internal explosion [11,12], dielectric elastomer actuation [13], magnetic navigation [14], onsite flow battery energization [15] and actuation via induced energy gradients [16]. Among these, soft magnetic robots, inheriting the advantages from traditional rigid magnetic actuation [17], stand out due to their excellent performance in a confined space with relatively facile control strategies and rapid responses. Thanks to the well-established magnetic control strategies and infrastructures [18], these devices significantly lower the learning curve and allow developers to focus their efforts on new feature developments that can be applied readily in practice.

Recently, a number of studies on soft magnetic robots have been reported [19-32]. These robots achieved advanced locomotion and various functionalities in enclosed, unstructured environments and some challenging applications, e.g., in targeted drug delivery [19-21] and in minimally-invasive surgery [22]. Targeted for biomedical applications, magnetic particles were introduced into soft matrix such as soft elastomers [23], hydrogels [24-26] and composites [27], and have been demonstrated in the applications for various manipulations at micro scale. Recently, a soft magnetic robot with a multi-legged design was shown to exhibit rapid locomotion in a harsh environment [29].

Remarkably, such accurately presetting of the addressable internal magnetic domains in soft bodies paves a new way to precisely control the dynamic motion of soft robots and offers them new opportunities to achieve complex gaits [30-32]. For instance, utilizing high compliance of soft materials, Sitti's group showed a continuously-magnetized soft robot that can achieve a multimodal locomotion [30]; nearly in the same period, Zhao *et al* reported an elegant 3D printing technique and build discrete magnetized ferromagnetic domains demonstrating complex shape changes [31]. However, to further exploit their potential and equip new capabilities towards higher level intelligence [30,33], it is very necessary to codesign magnetic actuation strategy with other functionalities, and further to heterogeneously integrate various functional parts into a configurable magnetic robot system [34-37], e.g., constructing a magnetic robot system with a specific magnetized and shaped profile and both integrated with other desirable heterogeneous functional components. Especially when those functional components can be obtained conveniently from diverse advanced manufacturing techniques, including but not limited to 3D printing, soft lithography, laser processing, molding and even transfer printing. However, physical implementation of such sophisticated soft magnetic robot has been hindered by lack of a facile yet universal manufacturing route that can fully take advantages of various manufacturing techniques, flexibly configure soft magnetic robots and integrate totally different functional units for desirable specifications as that LEGO® toys do. Therefore, one desirable solution is to preset magnetic domains as "LEGO strategy": a), design a few specific basic magnetized vector cells or functional cells in specific shapes serving as basic cells; and then b), configure a modularized robot system in various temporal sequences and spatial forms with diverse configurations to achieve various capabilities/functions in a cost- yet time-efficient way.

Transfer printing is a set of techniques for 2D and 3D discrete rearrangement of various material or functional parts spatially from a donor to a receiver [38]. As a versatile platform technology, it offers a useful yet flexible tool for fabricating a high-performance, heterogeneously integrated functional system at a relatively low cost. During the transfer process, the energy release rate between the transfer stamp and the donor/receiver substrate plays a critical role. Thus, successful implementation usually relies on precisely tuning such energy release rates [38]. Previously, various theoretical and experimental methods were reported using different tuning approaches [39-41], e.g., using various micro structures or kinetical controlling [42-46]. However, these transfer printing mechanisms usually results in a narrow operational window, hindering fast transfer of the knowledge to other groups that are likely to use them. Further, most of these transfer techniques often lack selectivity, and patterning selection is necessary during prior preparations, e.g., optical lithography and corresponding chemical/physical etching, which makes the process technically complicated and hence lower the success rate. By tuning the adhesion of the stamp via an amide embedment [47] and using the stamp as a receiver simultaneously, we presented a simple transfer printing technique that can achieve selective transfer of desired patterns [48]. However, such an adhesion tuning is a bit time-consuming, and the selection strictly based on pattern line width limits its widespread applications. Hence, a better tuning strategy with broad operational window and more general selective transfer printing mechanism would significantly enhance its efficiency and applicability.

Inspired by LEGO® toys, by utilizing a newly-developed laser-tuned selectively adhesive transfer printing of modularized heterogeneous (e.g. pre-anisotropic magnetized ferromagnetic and other functional) cells, we propose an elegant yet flexible approach to configure 3D discretely-magnetized multifunctional soft robots. With the newly presented method, we demonstrate a wide range of soft magnetic robots, including 2D/3D magnetized, 2D/3D shaped, heterogeneous responsive, multi-field responsive, environment perception, multi-function integration and even functional updating, repairing and recombination of daughter robots. Furthermore, a few possible application scenarios were demonstrated, such as precisely assembling an LED with micron-scale electrodes onto a circuit in a confined space (height of 2 mm, Movie S1) and carrying out drug delivery with a certain trafficability and steering in a wet and unstructured condition that mimicked a gastric environment (Movie S2). As a simple yet effective technique, our fabrication method may offer researchers an extra toolbox to preset 2/3D discrete magnetic domains and achieve various functional integration towards intelligent soft robots.

2. Results and discussion

As mentioned earlier, a selective transfer of desired width pattern was developed by our group recently. However, when we try to use this technique to make a configurable soft robot as LEGO® toys do, such a selective mechanism on width severely constrains freedom in robot design. A more general selective transfer printing is urgently needed. Surprisingly, as shown in Fig. 1a, we found that by selectively surface ablating an elastomeric stamp/film using different operational parameters, it can selectively lead to diverse local surface morphologies. Based on such a principle, the corresponding practical contacting surface area and hence its adhesion, can consequently change the energy release rate between the interfaces, Fig. 1b, instead of relying on the peeling speed and other factors. Such a surface adhesion tuning mechanism potentially provides a strategy for selective transfer printing. Furthermore, leveraging the external magnetized magnetic field, ferromagnetic particles can be arranged in an orderly queue in elastomer matrix and hence perform an anisotropic magnetism (Fig. 1c). Combining such a laser-tuned selectively adhesive transfer printing and laser cut pre-anisotropic magnetized ferromagnetic silicone cells, as shown in Fig. 1d and e, we present here a simple yet effective way to fabricate 2/3D discretely-magnetized configurable soft robots with a 2/3D shape on a sacrificial 2/3D substrate (more details, refers to the following and Experimental section), as well as extensive heterogeneous integration of other functional modules via transfer printing of desirable functional cells.

2.1. Laser-tuned selectively adhesive transfer printing and soft robot fabrication

Initially, thin neodymium-iron-boron (NdFeB) microparticles embedded ferromagnetic silicone films are prepared by scraper scraping a thin layer of thoroughly mixed PDMS-prepolymer with NdFeB microparticles on a flat support. The internal magnetic domains in such a ferromagnetic particle embedded silicone film that is in a semi-cured state can be bulkily reoriented and then fixed upon fully cured in any arbitrary directions by aligning a parallel magnetic field (Fig. 1c and d). With a high-power lasing, the cured, anisotropic magnetized film can be cut into any arbitrary planar patterns. Surprisingly, as shown in Fig. 1a, when we tried to use a relatively low power laser to scan the surface, we found that the surface morphology of the magnetized film can be altered and tuned by varying the laser operational parameters. That means, the adhesion and corresponding energy release rate between a silicone made stamp and pre-pattern-cut magnetized film can also be tuned to satisfy the physical requirements during transfer printing (Fig. 1b, more detailed mechanism investigation, please refer to the following subsection). More importantly, such a laser-tuned surface morphology/adhesion mechanism removes the constraints on pattern width in the previous developed approach, hence can serve as a general strategy to transfer any desired patterns.

Serving as basic pre-anisotropic magnetized ferromagnetic cells, any pre-cut specific patterns can be selectively picked up from the donor and transfer printed onto a receiver while undesirable patterns remain on the donor after the surface morphologies are selectively altered. According to the previous work [30-32], precisely presetting (encoding) of magnetic domains inside silicone cells is of great importance in the construction of high-performance magnetic robots. Through a proper tuned predesigned temporal sequence or spatial alignment/configuration of a multiple transfer printing, a soft magnetic robot structure with discrete preset magnetic domains can be obtained on a temporary (e.g. water-soluble) receiver (Fig. 1e). After that, the adjacent cells were spliced before releasing from the receiver by removing the temporary receiver and a magnetic robot was formed finally (Movie S3). Owing to good compliance of silicone cells, the receiver can either be planar or 3D shaped. Therefore, 2/3D shaped robots can be obtained by a proper alignment of the pre-anisotropic magnetized ferromagnetic silicone cells and the corresponding design of soluble sacrificial receivers (Fig. 1e).

Unlike on-demand magnetization strategies, our procedure homogeneously magnetizes the entire film which may potentially enable large-area parallel manufacturing, and the direction of internal magnetic domains can also be adjusted during laser patterning and transfer printing process. That is, the combination of original magnetization, laser patterning and cells alignment determine the final internal magnetic domain configuration. Such a magnetization strategy is a flexible configuration method and can effectively prevent magnetization interfere during the whole process.

2.2. Mechanism of surface adhesion tuning and selectively transfer printing

During the transfer printing process, silicone cells should be picked up from a donor and then printed onto a receiver. According to transfer printing theory, the surface adhesion/energy release rate between the donor, receiver and stamp should satisfy the following criteria:

$$G^{\text{stamp/cells}} > G^{\text{donor/cells}} \quad \text{for pickup} \tag{1}$$

$$G^{\text{receivers/cells}} > G^{\text{stamp/cells}} \quad \text{for printing} \tag{2}$$

As shown in Fig. 1b, the energy release rate between stamp and cells should be tuned in an appropriate range: greater than the energy release rate of weak interface between cells and donor for picking up, and less than the energy release rate of strong interface between cells and receivers for printing.

As found in this work, the energy release rate between the pre-pattern-cut cells and stamp can be tuned by surface morphology control, e.g., via UV lasing the stamp or patterned magnetic cell surface. In practice, such a control can be implemented by varying a few laser operational parameters. Fig. 2a shows the effect of laser scanning speed *v* and scanning line spacing *d* on the surface roughness of a stamp. With a decrease in scanning speed or lasing line spacing, the surface changed from smooth to rough (Fig. 2a and S1). This is consistent with the profile observed in the images obtained using an ultra-depth three-dimensional optical microscope (Fig. S2). Furthermore, we systematically studied the effects of laser scanning speed and scanning line spacing on the energy release rate of the interface between the magnetic film and transfer stamp by following a previously developed protocol.

It is well-known that the "sticky" contact surface plays an important role in surface adhesion that relies on van der Waals force and this was verified in the previous study [49]. Since we used silicone-based materials to make the transfer stamp as well as the transferred cells, it is hypothesized that the effective contact area will be an important factor in the transfer process. Based on this hypothesis, we propose a mathematical model (Eq. 3) relating scanning speed, scanning distance of laser, and energy release rate to the effective sticky contact surface:

$$G = G_0\left[\left(\frac{(d-w)^2}{d^2}\right) + (\frac{2wd-w^2}{d^2})\left[\mathrm{k}\sin^{\mathrm{m}}\left(\frac{\pi v}{2\mathrm{v}_0}\right) + \mathrm{b}\right]\right] + \mathrm{e} \tag{3}$$

G_0, w, v_0 are the original energy release rate (~14 J/m^2), laser spot size (0.02 mm) and maximum scanning speed (2200 mm/s), respectively. By numerical fitting, the constants k, m, b and e in our situation can be determined resulting in:

$$G = G_0\left[\left(\frac{(d-w)^2}{d^2}\right) + (\frac{2wd-w^2}{d^2})\left[199 \times \sin^{0.779}\left(\frac{\pi v}{2\mathrm{v}_0}\right) - 123\right]\right] - 1.31 \tag{4}$$

According to Eq. 4, we can tune the surface adhesion with appropriate laser parameters during transfer printing implementation (Fig. S3) under the guidance of surface energy release theory (Fig. 1b).

Notably, during the transfer printing process, the energy release rate between the cells and donor was relatively low, which results in a weak interface between the cells and donor. Hence, the cells on the donor are prone to be picked up by the stamp. Meanwhile, the surface of dissolvable receiver is sticky, the pre-pattern cells can be transfer printed onto the receiver from the stamp. Therefore, by tuning the surface morphology of stamp and hence to its adhesion in an appropriate range, it offers a new method to achieve transfer printing in a simple way. More importantly, the surface morphology and adhesion of stamp can be modified on demanded on any specific zones with a laser scanning adjustment. Hence, the surface morphology can directly determine whether ferromagnetic silicone cells being picked up or not, combining the laser cutting. Consequently, utilizing this principle, we can easily achieve a selective adhesive transfer printing coupling laser patterning and operational parameter tuning. Similarly, such a strategy can be used on the surface morphology modification of the pre-anisotropic magnetized ferromagnetic films and hence the adhesion tuning as well.

As shown in Fig. 2c, we demonstrated such a selectively transfer print of a magnetic butterfly by tunable surface adhesion. The pre-cut stickier butterfly cell was selectively picked up and transfer printed onto the receiver by a stamp while roughened parts remained on the donor (more details, refer to Movie S4). Further, a parallel transfer printing and following splicing of two identical magnetic response rays were also accomplished employing two industrial robots (Fig. 2d and Movie S5), showing the capabilities of this technique for automatically and parallelly fabricating magnetic robots.

2.3. Magnetization characterization

To systematically study the effect of various factors on the response characteristics of ferromagnetic silicone cells that are subjected to magnetic fields [50]. We measured the deflection angle (θ) of ferromagnetic silicone cells as a function of magnetic flux density with a characterization platform (Fig. 3 and S4). As expected, we found that thinner and longer geometrical dimensions induce a greater deflection of ferromagnetic silicone cells because of decreasing structural stiffness (Fig. 3a). Also, the effect of various ratios of PDMS-prepolymer (silicone base/curing agent) on the response of magnetized cells was explored. As the ratio increased, the stiffness of the magnetized cells decreased [51], so that greater deflection occurred under the same magnetic flux density (Fig. 3b). However, excessive ratios will lead to too soft and sticky structures which are susceptible to mechanical damage. In addition, we also studied the effect of ferromagnetic particle (NdFeB) concentrations on ferromagnetic silicone cell response. As shown in Fig. 3c, when the ratio of PDMS base and NdFeB particles was 1:2, magnetized cells reached peak deflection. We found higher concentrations will enhance the stiffness of the structure thus decreasing deflection for the same magnetic flux density.

In practice, film-formation and curing on glass slides is prone to produce obvious structural anisotropy and residual stresses for this kind of membrane structure. Therefore, ferromagnetic silicone cells tend to deflect more in one direction than the other in equal and opposite magnetic fields, hence leading to relatively large errors as shown in Fig 3c. When the ratio of PDMS silicone base to NdFeB particles was high (2:1), the magnetic torque-induced force is very low and thus the structural anisotropy and residual stresses have a larger impact on magnetic response. In contrast, when the concentration of magnetic particles is larger, the error induced by residual stresses is smaller because the magnetic torque-induced force assumes a larger role.

We further studied the effect the magnetized magnetic field. Stronger magnetized magnetic fields can produce better magnetization and show a better magnetic response under the same actuation magnetic fields (Fig. 3d). Additionally, the cross-section of pre-anisotropic magnetized ferromagnetic film was observed under the field scanning electron microscopy (FSEM) (Fig. S5). We also found that precuring times also affect the particle distribution, as revealed by energy-dispersive X-ray spectroscopy (Fig. S6). With increasing precuring time, the distribution of ferromagnetic particles was more uniform, resulting in a slightly higher magnetic torque-induced deflection (Fig. 3e and f).

2.4.Configurable soft magnetic robots

Configurable robots have high versatility and demonstrate stronger adaptability in different environments, and their operational modes can be switched or functional modules can be added or updated when needed [52]. Similarly, configurability is a desirable character for microrobots, too, to flexibly assemble target microrobots according to specific designs. Utilizing the newly-developed transfer printing method, various soft magnetic robots/structures with diverse shaped and magnetized profiles can be flexibly obtained. Here demonstrated a serial of soft magnetic robots with specific magnetic domains and shape profiles that transfer printed with various magnetic cells.

Reprocessable and repairable features are also desirable in many scenarios [53]. Here, by simply reassembly three more arms on a tripod robot, leveraging this transfer printing-based method in Fig. 4, a and b, it can function as a weight-lifting robot being able to lift a cargo (0.05 g) up to 5 times of its own weight (Fig. 4, c and d). What's more, the weight-lifting robot can be repaired by replacing the unnormal cells leveraging laser cutting and retransfer printing, a desirable feature if local degaussing/damage should occur, Fig. 4e-h. Since the pre-anisotropic magnetized ferromagnetic cells can be selectively transferred onto shape alterable sacrificial receivers, our technique is capable of combining 3D shapes or/and 3D discrete magnetization as demanded by some particular applications. As shown in Fig. 4i, a series of magnetic 2/3D shaped structures with 2/3D magnetization have been realized and show specific response behaviors.

Besides the above flexible alignment and combination of discrete pre-anisotropic magnetized cells, our strategy can be extended to robot combination and reconfiguration from a few modular (daughter) robots targeted for various behaviors. As shown in Fig. 4j, based on the same honeycomb gridded structure with an opposite alignment of magnetized cells (afferent, α type, and afferent, β type, to its geometrical center), we configure them with different combinations (evenly circumferential distributed three α type daughter robots with inner tips spliced together, triangular distributed three α type daughter robots with tips spliced together, stacked α type and β type daughter robots with outer tips spliced together, 60° shifted stacked α type and β type daughter robots with centers spliced together) to obtain various behavioral magnetic robots, Fig. S7 and Movie S6. under a same external magnetic field, they showed totally different behaviors and motion patterns, although they were made from the homologous daughter robots. Connection forms and fixed constraints between daughter robots also play an important role in controlling the motion of robots subjected to external magnetic fields. For instance, just shifting the connection points, the robots showed totally different behavior in a same external driven magnetic field. More potential motions can be achieved by varying assembly alignment and fixed constrains based on such kind of daughter robots.

2.5. Heterogeneous integration towards multifunctional soft magnetic robots

Heterogeneous integration of different functional parts into a robotic system is an effective way to achieve more sophisticated and controllable response behaviors [54], such as gradient-response, multi-field actuation, actuation and perception integration and so on. In our transfer printing processes, the transferred targets can be easily substituted, and it brings a native advantage for heterogeneous integration of diverse functional cells. Utilizing this feature, abundant functional cells fabricated by a variety of advanced manufacturing methods can be transfer printed in a robotic system at a low cost, which significantly extends the fabrication flexibilities and abundance of soft magnetic robots.

With a different concentration of ferromagnetic particles and pattern shapes as shown in Fig. 5a-c, we made a heterogeneous magnetically-responsive flower-like structure by mimicking stamens, petals, and leaves of a true flower. Under the same actuation situation, the corresponding magnetic cells show a different bending response (Fig. 5d-f). As shown in Fig. 5g and Movie S7, it can mimic the open and close processes like a true dandelion flower with a single relatively uniform actuation magnetic field.

Multi-field actuation, self-sensing and environment perception are also attractive attributions for small-scale robots, as showing in the previous work [55,56]. For example, Nelson *et al* reported an ingenious soft micromachine with programmable motility and morphology. The compound bodies can respond to external magnetic signals for mobility and spatiotemporally controlled heating signals for shape shifting [55]. Besides heterogeneous magnetically-responsive cells, we further integrate the cells with totally different materials and actuation mechanism to realize multi-field actuation. A multi-field responsive robot with magnetic cells and shape memory polymer (SMP) cells was achieved with two independent actuations (Fig. 5, h and i, Movie S8). The thermal stimulus actuates the SMP cells to recover its initial shape and subsequently the magnetic stimulus actuates the magnetic cells to deform, which is mutually independent and will not interfere with each other. For multifunctional heterogeneous integration, we seamlessly transfer print the actuation cells and sensor cells into a robot, Fig. 5j and Movie S9. There, a three-legged robot is integrated with 3 actuation magnetized cells and a temperature sensor cell. The robot can locomote and detect the ambient temperature real-timely by indicating different colors (orange red on cold surface and yellow on the hot surface). Moreover, other functions can also be integrated into a robot system for more complex tasks including but not limited to actuation, sensor, active signaling/interaction, energy harvesting/storage/management and computing/control cells. Since these diverse functional cells with various materials, structures or functions may be obtained conveniently with most suitable fabrication techniques, the transfer printing method can provide a general platform technique to heterogeneously integrate these functional cells into a soft magnetic robot for a specific application or scenario in practice. Consequently, this method can maximize the advantages from all kinds of materials, structures or functions with corresponding fabrication techniques, fully utilizing the specialties of these techniques for sophisticated robot implementation in a reasonable cost at present stage.

2.6.Application demonstrations

To explore the potential applications of soft magnetic robots, we further develop several specific configured magnetic robots, working in several unstructured environments and demonstrating their corresponding capabilities. We are excited that it is easy to directly obtain a hollow sealed ultrathin structure on a soluble sphere receiver. Such a hollow sealed ultrathin 3D structure with specific magnetization profiles is costly to make with other fabrication techniques. This 3D shaped structure with 3D continuous and discrete magnetization and can be actuated under varying actuation magnetic fields (Fig. 6a). Furthermore, such a kind of hollow sealed ultrathin structure can be utilized to mimic the rolling mode of the tumbleweed, and provides a solution for a robot to pass through an unstructured and harsh gastric environment. As shown in Fig. 6b and Movie S2, targeted drug delivery can be accomplished with few obstacles in such a condition. This tumbleweed robot shows omnidirectional motion and pass-ability in such a gastric bumpy model filled with water in a rolling mode. What's more, it has a high empty volumetric factor (92.8%) and hints it potentially allows for relatively high volume for cargo load.

Besides the tumbleweed inspired robot, we also developed an inchworm-liked robot and a three-legged robot. Their linear locomotion characteristics have been discussed in the Supplementary Materials and figures (Fig. S8 and S9). The inchworm-like robot can walk steadily in an S-shaped tube with an inner diameter of 8 mm (Fig. S8). Further, in this configuration of the inchworm-like magnetic robot that is heterogeneously integrated using our method, its none responsive planar cell can provide a relatively stable bearing platform in movement. We found that under a tight, confined environment, it can carry an LED with micron-scale electrodes into the confined space with height of about 2 mm and assemble it onto a functional circuit and turn on the circuit by precisely assembling an LED on liquid metal circuits (Fig. 6c-f, Fig. S10 and Movie S1), indicating its potential applications in ultrafine assembly in the future.

2.7. Discussion

Compared with the previous works, the advantages of our method are mainly reflected in the following aspects. First, it is easy for flexibly presetting magnetic domains since the ferromagnetic particles can be re-orientated in an arbitrary 3D direction during magnetization process (additionally, laser cutting patterning and alignment can also tune the magnetic domains). Alternatively, we can also achieve a 3D shape by aligning the discrete magnetized cells on an arbitrarily-shaped temporary receiver and further flexibly combine 2D/3D shapes and 2D/3D magnetization profiles as demanded. Second, it is easier for heterogeneous integration of various function/material cells to obtain more sophisticated behaviors, and undesirable cells or daughter robots can be quickly replaced/updated/recombined by retransfer printing (the detailed characteristic comparison with existing methods was shown in Supplementary Table S1 in the Supplementary Materials). However, with our present fabrication facility, the lower bound limit of constructed robots is around submillimeter scale. Smaller scale and more sophisticated robots could be configured with further material/process optimization or/and advanced fabrication facility with higher precision. Furthermore, more heterogeneously-integrated, functional synergistic soft magnetic robots can be further studied towards higher intelligent and performance in the future.

More importantly, small scale soft robots are often preferably reconfigured in real time and programmed online in many specific applications, e.g., previously demonstrated camouflaging soft robots [57], shape-morphing micromachines with an in situ reprogrammable strategy [58] and a swarm robotic system based on loosely coupled component [59]. Under the existing circumstance, our method, majorly, is an offline strategy like LEGO's, providing a feasible solution for making modularized soft magnetic robots with a flexible configuration and working modes shifting. With further investigation and development, we believe such a technique will be helpful to develop a robot that can highly adapt to their immersed complex environments via introducing the real-time reconfiguration and re-programming mechanisms of both actuated and functional modules in the future.

3. Conclusions

By introducing a surface adhesion tuning mechanism derived from laser surface morphology alteration and establishing its theoretical adhesion model, we developed a facile transfer printing-based technique for flexible fabrication of multifunctional soft magnetic robots. This method enables rapid fabrication of soft magnetic robots in a configurable way and makes it easier for heterogeneous integration of diverse functions. Particularly, via systematic experiments and theoretical modeling, we revealed the influence mechanisms of laser treatment under different parameter settings on the surface morphology and thus its surface adhesion of flexible silicone film substrate. The magnetized cells can be specific directly and selectively split, transferred and subsequently printed to make a robot simply by varying laser parameter settings. This method can be a versatile platform technique for flexibly configuring soft magnetic robots with specific shaped and magnetized profiles, and enabling the heterogenous integration of totally different functional cells for constructing sophisticated magnetic robots.

4. Experimentals

4.1. Preparation of the ferromagnetic silicone cells

The magnetic robots consist of two kinds of cells: magnetic cells and connecting cells, respectively. The magnetic cells were made by mixing commercial silicone elastomer (Sylgard 184, silicone base/curing agent 20 g: 1 g, Dow Corning, USA) with 40 g ferromagnetic particles (MQFB-B-20076-089, Magnequench, USA). The connecting cells were made by mixing the commercial silicone elastomer with carbon black (XC72R, Cabot, USA) from Alibaba at a weight ratio of 10: 1: 0.05 (silicone base: curing agent: carbon black). The detailed processes are described as following: First, the ferromagnetic particles, silicone base, and curing agent were stirred by digital stirring (RW 20, IKA, Germany) at 2000 RPM for 3 min. Second, the mixture was vacuumed to remove bubbles. Third, the mixture was bladed into a thin film. Fourth, the thin film was precured at 75°C for 5 min in an oven (UF 55 plus, Memmert, Germany) to increase its viscosity and avoid the ferromagnetic particle accumulating in the two sides in magnetization process. Specifically, to visualize different parts of dandelion flower-like structure such as stamens, petals and leaves, various dyes were added in the PDMS mixture.

4.2. Preparation of the stamp and the donor/receiver substrate

The stamp was prepared via mixing PDMS (Sylgard 184, silicone base/curing agent 30 g:1 g) with 3 g of nano reduced iron powder. First, the silicone, curing agent and nano reduced iron powder were stirred by a digital stirring at 2000 rpm for 3 min. Second, the mixture was bladed casted into a thin film of 1000 μm after vacuumed for removing extra bubbles. Third, the film was cut as a stamp and the surface of the stamp was ablated to tune its adhesion by a UV laser maker (HGL-LSU3/5EI, Huagong Laser, Wuhan, China) with a pulse frequency of 80 kHz, pulse width of 0.2 μs, and working current of 33.5 A. the donor is a release paper peeled off from adhesive stickers (Tango, A4, Alibaba, China). The planar receiver was made of the water-soluble tape (ASWT-1, Aquasol, USA) and the 3D receiver is customized by a 3D Printer using polyvinyl alcohol (PVA) soluble filament from Alibaba.

4.3. Magnetization, patterning, transfer printing and splicing

The semi-cured thin nonmagnetic film was magnetized under the parallel magnetic field produced by a pair of planar magnets (N35-NdFeB purchased from Alibaba, about 2500 Gs surface flux) in the oven at 75°C for 40 min. Then, the magnetized film was full-cured on a programmable heating platform (PR5-3T, Harry Gestigkeit, Germany) at 90°C for 30 min. Finally, the magnetized film was cut into various magnetized cells and selectively treated to tuning the adhesion according to the design by the UV laser maker with a pulse frequency of 80 kHz, pulse width of 0.2/0.1 μs, and working current of 33.5 A. Ferromagnetic silicone cells were selectively picked up by the stamp and printed on the temporary receiver. The assembly of magnetic robots can be achieved by multiple splicing discrete magnetic cells into an entity on a supportive receiver. The interfaces between the adjacent cells were spliced by a superglue (7146, Deli, China). to quantitatively characterize the response of magnetic cells, all cells are cut into specific rectangular cells (thickness of 0.2 mm, length of 5 mm and width of 2 mm in Fig. 3b-d, thickness of 0.2 mm, length of 8 mm and width of 2 mm in Fig. 3e).

4.4. Optical characterization

A metallographic microscope (BA310MET-T, Motic, Xiamen, China) with a CCD camera was used to observe the direction state of the Ferromagnetic particles in the liquid PDMS matrix. An ultra-depth three-dimensional microscope (DXS 510, Olympus, Japan) was used to characterize the surface roughness of the stamp scanned by the laser under different parameters. The response of the magnetic robots or structures were recorded by a digital camera (Canon EOS 70D, Tokyo, Japan). The distribution of the ferromagnetic particles in the cured PDMS matrix was observed by a field scanning electron microscope (FSEM, GeminiSEM300, Garl Zeiss, Germany) through the cross section. The response characteristics of quadrate magnetic cells was recorded by an industrial USB microscope (A1, Andonstar, China) under specific magnetic fields.

4.5. Sample preparation and test methods for Energy release rate measurement

Sample preparation: first, a thin film of release paper was stuck onto the surface of a smooth aluminum plate. Second, the magnetic PDMS composite was bladed into a thin layer (thickness: 200 μm) on the Polyethylene terephthalate film (YH-2910, Shanghai Yunhao, China) and consequently cured at a 75°C for 40 min in the oven and at 90°C for 30 min on the heating platform for totally curing. Third, the cured magnetic film on the PET film was cut into a specific pattern by the UV laser marker finally being attached uniformly to the donor surface. A standard customized roller was used to ensure the attachment tightly and evenly, and then the sample for measuring the energy release rates of the interface between the magnetic film and donor was ready for the energy release rate measurement. The same method is used for preparing the sample of stamp and planar receivers for characterizing the interface of magnetic film/stamps and magnetic film/receivers; Energy Release Rate Measurement methods: the energy release rate measurement setup was based on the international standard test method for 90° peeling resistance of energy release rate (Designation: ASTM D 6862-2004) and test method for peeling strength of pressure-sensitive tape (Designation: GB/T 2792-1981).

4.6. Fabrication methods and experimental settings in demonstrations

For Automatically parallel assembly of two magnetic rays, the pre-anisotropic magnetized film was patterned and surface treated by laser with different operational parameters. Two identical ray cells were selectively transferred printing on a planar soluble receiver by an industrial robot (KR3, R540, KUKA, Germany). And the junctions were spliced with glue by a 3-axis automated fluid dispensing robot (SM 200DS, Musashi, Japan); For Assembling LED in a confined space and targeted drug delivery: a rectangle NdFeB magnet (100 mm × 50 mm × 20 mm, N52, about 2200 Gs surface flux, Alibaba) was used to generate magnetic fields required for actuation; For configuration of homologous daughter robots: all combined gridded structures were actuated in a water environment and show the different behaviors and motion patterns due to their different alignment and constraints; For multi-field responsive robot: the robot was integrated with magnetic actuation cells and thermal actuation cells that was printed by commercially available 3D FDM printer directly with SMP filament; For Heterogeneous integration of actuation cells and sensor cell: the actuation cells were made of pre-anisotropic patterned magnetized silicone cells (PDMS base: cross-linking agent: NdFeB=20: 1: 40 g). the temperature sensor was made of a patterned PDMS film coated with a thermochromic pigment (720-QT-004-10, Angelus Shoe Polish, USA) which was red in cold environment and yellow in warm environment (more than 28°C); For targeted drug delivery: a polyvinyl chloride model stomach (160 mm × 110 mm × 55 mm) filled with water was used to mimic unstructured stomach environment, and a tumbleweed-inspired robot was actuated for targeted drug delivery in such environment under the external magnetic fields. (Fabrication of the ultrathin 3D sealed structure: first, they were assembled by multiple splicing discrete magnetized cells on a dissolvable 3D receiver. Then, adjacent cells were spliced by a superglue. Finally, the temporary receiver was dissolved by water to gain the independent 3D structure); For locomotion and assembling process, the direction and intensity of the applied magnetic fields were varied by manually manipulating the magnet to change its position and orientation according to the specific situation.

References

[1] H. Ding, X. Yang, N. Zheng, M. Li, Y. Lai, H. Wu, Tri-Co Robot: a Chinese robotic research initiative for enhanced robot interaction capabilities, *Natl. Sci. Rev.* 5 (2018) 799–801.

[2] G. Z. Yang, J. Bellingham, P. E. Dupont, P. Fischer, L. Floridi, R. Full, N. Jacobstein, V. Kumar, M. McNutt, R. Merrifield, B. J. Nelson, B. Scassellati, M. Taddeo, R. Taylor, M. Veloso, Z. L. Wang, R. Wood, The grand challenges of science robotics, *Sci. Robot.* 3 (2018) eaar7650.

[3] D. Rus, M. T. Tolley, Design, fabrication and control of soft robots, *Nature* 521 (2015) 467–475.

[4] C. Lee, M. Kim, Y. J. Kim, N. Hong, S. Ryu, H. J. Kim, S. Kim, Soft robot review, *Int. J. Control. Autom. Syst.* 15 (2017) 3–15.

[5] C. Majidi, Soft Robotics: A Perspective - Current Trends and Prospects for the Future, *Soft Robot.* 1 (2014) 5–11.

[6] C. Laschi, B. Mazzolai, M. Cianchetti, Soft robotics: Technologies and systems pushing the boundaries of robot abilities, *Sci. Robot.* 1 (2016) eaah3690.

[7] L. Hines, K. Petersen, G. Z. Lum, M. Sitti, Soft Actuators for Small-Scale Robotics, *Adv. Mater.* 29 (2017) 1603483.

[8] G. Gu, J. Zou, R. Zhao, X. Zhao, X. Zhu, Soft wall-climbing robots, *Sci. Robot.* 3 (2018) eaat 2874.

[9] S. I. Rich, R. J. Wood, C. Majidi, Untethered soft robotics, *Nat. Electron.* 1 (2018) 102–112.

[10] M. Wehner, R. L. Truby, D. J. Fitzgerald, B. Mosadegh, G. M. Whitesides, J. A. Lewis, R. J. Wood, An integrated design and fabrication strategy for entirely soft, autonomous robots, *Nat. Publ. Gr.* 536 (2016) 451–455.

[11] R. F. Shepherd, A. A. Stokes, J. Freake, J. Barber, P. W. Snyder, A. D. Mazzeo, L. Cademartiri, S. A. Morin, G. M. Whitesides, Using explosions to power a soft robot, *Angew. Chemie - Int. Ed.* 52 (2013) 2892–2896.

[12] M. T. Tolley, R. F. Shepherd, M. Karpelson, N. W. Bartlett, K. C. Galloway, M. Wehner, R. Nunes, G. M. Whitesides, R. J. Wood, An untethered jumping soft robot, in *IEEE/RSJ International Conference on Intelligent Robots and Systems* (ICIRS, 2014), pp. 561–566.

[13] T. Li, G. Li, Y. Liang, T. Cheng, J. Dai, X. Yang, B. Liu, Z. Zeng, Z. Huang, Y. Luo, T. Xie, W. Yang, Fast-moving soft electronic fish, *Sci. Adv.* 3 (2017) e1602045.

[14] C. Bi, M. Guix, B. V. Johnson, W. Jing, D. J. Cappelleri, Design of microscale magnetic tumbling robots for locomotion in multiple environments and complex terrains, *Micromachines* 9 (2018) 68.

[15] C. A. Aubin, S. Choudhury, R. Jerch, L. A. Archer, J. H. Pikul, R. F. Shepherd, Electrolytic vascular systems for energy-dense robots, *Nature* 571 (2019) 51–57.

[16] L. X. Lyu, F. Li, K. Wu, P. Deng, S. H. Jeong, Z. Wu, H. Ding, Bio-Inspired Untethered fully soft Robots in Liquid Actuated by Induced Energy Gradients, *Natl. Sci. Rev.* 6 (2019) 970-981.

[17] S. Bouchebout, A. Bolopion, J. O. Abrahamians, S. Régnier, An overview of multiple DoF magnetic actuated micro-robots, *J. Micro-Nano Mechatronics*. 7 (2012) 97–113.

[18] T. Xu, J. Yu, X. Yan, H. Choi, L. Zhang, Magnetic actuation based motion control for microrobots: An overview, *Micromachines* 6 (2015) 1346–1364.

[19] O. Veiseh, J. W. Gunn, M. Zhang, Design and fabrication of magnetic nanoparticles for targeted drug delivery and imaging, *Adv. Drug Deliv. Rev.* 62 (2010) 284–304.

[20] S. Tottori, L. Zhang, F. Qiu, K. K. Krawczyk, A. Franco-Obregõn, B. J. Nelson, Magnetic helical micromachines: Fabrication, controlled swimming, and cargo transport, *Adv. Mater.* 24 (2012) 811–816.

[21] K. E. Peyer, L. Zhang, B. J. Nelson, Bio-inspired magnetic swimming microrobots for biomedical applications, *Nanoscale* 5 (2013) 1259–1272.

[22] Y. Kim, G. A. Parada, S. Liu, X. Zhao, Ferromagnetic soft continuum robots, *Sci. Robot.* 4 (2019) eaax7329.

[23] G. Z. Lum, Z. Ye, X. Dong, H. Marvi, O. Erin, W. Hu, M. Sitti, Shape-programmable magnetic soft matter, *Proc. Natl. Acad. Sci. U. S. A.* 113 (2016) E6007–E6015.

[24] I. M. El-Sherbiny, H. D. C. Smyth, Smart magnetically responsive hydrogel nanoparticles prepared by a novel aerosol-assisted method for biomedical and drug delivery applications, *J. Nanomater.* 2011 (2011) 910539.

[25] P. Ilg, Stimuli-responsive hydrogels cross-linked by magnetic nanoparticles, *Soft Matter* 9 (2013) 3465–3468.

[26] S. Park, S. Y. Ko, J.-O. Park, H. Li, G. Go, Magnetic actuated pH-responsive hydrogel-based soft micro-robot for targeted drug delivery, *Smart Mater. Struct.* 25 (2016) 027001.

[27] J. A.-C. Liu, J. H. Gillen, S. R. Mishra, B. A. Evans, J. B. Tracy, Photothermally and magnetically controlled reconfiguration of polymer composites for soft robotics, *Sci. Adv.* 5 (2019) eaaw2897.

[28] X. Yan, Q. Zhou, J. Yu, T. Xu, Y. Deng, T. Tang, Q. Feng, L. Bian, Y. Zhang, A. Ferreira, L. Zhang, Magnetite Nanostructured Porous Hollow Helical Microswimmers for Targeted Delivery, *Adv. Funct. Mater.* 25 (2015) 5333–5342.

[29] H. Lu, M. Zhang, Y. Yang, Q. Huang, T. Fukuda, Z. Wang, Y. Shen, A bioinspired multilegged soft millirobot that functions in both dry and wet conditions, *Nat. Commun.* 9 (2018) 3944.

[30] W. Hu, G. Z. Lum, M. Mastrangeli, M. Sitti, Small-scale soft-bodied robot with multimodal locomotion, *Nature* 554 (2018) 81–85.

[31] Y. Kim, H. Yuk, R. Zhao, S. A. Chester, X. Zhao, Printing ferromagnetic domains for untethered fast-transforming soft materials, *Nature* 558 (2018) 274–279.

[32] T. Xu, J. Zhang, M. Salehizadeh, O. Onaizah, E. Diller, Millimeter-scale flexible robots with programmable three-dimensional magnetization and motions, *Sci. Robot.* 4 (2019) eaav4494.

[33] M. Sitti, Miniature soft robots - road to the clinic, *Nat. Rev. Mater.* 3 (2018) 74–75.

[34] R. L. Truby, S. Li, Integrating chemical fuels and artificial muscles for untethered microrobots, *Sci. Robot.* 5 (2020) eabd7338.

[35] C. Ma, S. Wu, Q. Ze, X. Kuang, R. Zhang, H. J. Qi, R. Zhao, Magnetic Multimaterial Printing for Multimodal Shape Transformation with Tunable Properties and Shiftable Mechanical Behaviors, *ACS Appl. Mater. Interfaces* (2020), doi:10.1021/acsami.0c13863.

[36] J. A. C. Liu, J. H. Gillen, S. R. Mishra, B. A. Evans, J. B. Tracy, Photothermally and magnetically controlled reconfiguration of polymer composites for soft robotics, *Sci. Adv.* 5 (2019) eaaw2897.

[37] Q. Ze, X. Kuang, S. Wu, J. Wong, S. M. Montgomery, R. Zhang, J. M. Kovitz, F. Yang, H. J. Qi, R. Zhao, Magnetic Shape Memory Polymers with Integrated Multifunctional Shape Manipulation, *Adv. Mater.* 32 (2020) 1906657.

[38] A. Carlson, A. M. Bowen, Y. Huang, R. G. Nuzzo, J. A. Rogers, Transfer printing techniques for materials assembly and micro/nanodevice fabrication, *Adv. Mater.* 24 (2012) 5284–5318.

[39] H. Chen, X. Feng, Y. Huang, Y. Huang, J. A. Rogers, Experiments and viscoelastic analysis of peel test with patterned strips for applications to transfer printing, *J. Mech. Phys. Solids*. 61 (2013) 1737–1752.

[40] H. J. Kim-Lee, A. Carlson, D. S. Grierson, J. A. Rogers, K. T. Turner, Interface mechanics of adhesiveless microtransfer printing processes, *J. Appl. Phys.* 115 (2014) 143513.

[41] H. Cheng, M. Li, J. Wu, A. Carlson, S. Kim, Y. Huang, Z. Kang, K. -C. Hwang, J. A. Rogers, A viscoelastic model for the rate effect in transfer printing, *J. Appl. Mech. Trans. ASME.* 80 (2013) 041019.

[42] A. Carlson, H. J. Kim-Lee, J. Wu, P. Elvikis, H. Cheng, A. Kovalsky, S. Elgan, Q. Yu, P. M. Ferreira, Y. Huang, K. T. Turner, J. A. Rogers, Shear-enhanced adhesiveless transfer printing for use in deterministic materials assembly, *Appl. Phys. Lett.* 98 (2011) 26414.

[43] S. Y. Yang, A. Carlson, H. Cheng, Q. Yu, N. Ahmed, J. Wu, S. Kim, M. Sitti, P. M. Ferreira, Y. Huang, J. A. Rogers, Elastomer surfaces with directionally dependent adhesion strength and their use in transfer printing with continuous roll-to-roll applications, *Adv. Mater.* 24 (2012) 2117–2122.

[44] X. Feng, M. A. Meitl, A. M. Bowen, Y. Huang, R. G. Nuzzo, J. A. Rogers, Competing fracture in kinetically controlled transfer printing, *Langmuir* 23 (2007) 12555–12560.

[45] M. A. Meitl, Z. T. Zhu, V. Kumar, K. J. Lee, X. Feng, Y. Y. Huang, I. Adesida, R. G. Nuzzo, J. A. Rogers, Transfer printing by kinetic control of adhesion to an elastomeric stamp, *Nat. Mater.* 5 (2006) 33–38.

[46] T. H. Kim, A. Carlson, J. H. Ahn, S. M. Won, S. Wang, Y. Huang, J. A. Rogers, Kinetically controlled, adhesiveless transfer printing using microstructured stamps, *Appl. Phys. Lett.* 94 (2009) 113502.

[47] S. H. Jeong, S. Zhang, K. Hjort, J. Hilborn, Z. Wu, PDMS-Based Elastomer Tuned Soft, Stretchable, and Sticky for Epidermal Electronics, *Adv. Mater.* 28 (2016) 5830–5836.

[48] P. Peng, K. Wu, L. Lv, C. F. Guo, Z. Wu, One-Step Selective Adhesive Transfer Printing for Scalable Fabrication of Stretchable Electronics, *Adv. Mater. Technol.* 3 (2018) 1700264.

[49] S. Zhang, B. Wang, J. Jiang, K. Wu, C. F. Guo, Z. Wu, High-Fidelity Conformal Printing of 3D Liquid Alloy Circuits for Soft Electronics, *ACS Appl. Mater. Interfaces*. 11 (2019) 7148–7156.

[50] R. Zhao, Y. Kim, S. A. Chester, P. Sharma, X. Zhao, Mechanics of hard-magnetic soft materials, *J. Mech. Phys. Solids*. 124 (2019) 244–263.

[51] R. Seghir, S. Arscott, Extended PDMS stiffness range for flexible systems, *Sensors Actuators, A Phys.* 230 (2015) 33–39.

[52] P. Moubarak, P. Ben-Tzvi, Modular and reconfigurable mobile robotics, *Rob. Auton. Syst.* 60 (2012) 1648–1663.

[53] B. Zhang, K. Kowsari, A. Serjouei, M. L. Dunn, Q. Ge, Reprocessable thermosets for sustainable three-dimensional printing, *Nat. Commun.* 9 (2018) 1831.

[54] H. Lu, Y. Hong, Y. Yang, Z. Yang, Y. Shen, Battery-Less Soft Millirobot That Can Move, Sense, and Communicate Remotely by Coupling the Magnetic and Piezoelectric Effects, *Adv. Sci.* 7 (2020) 2000069.

[55] H. W. Huang, M. S. Sakar, A. J. Petruska, S. Pané, B. J. Nelson, Soft micromachines with programmable motility and morphology, *Nat. Commun.* 7 (2016) 12263.

[56] W. Jing, D. Cappelleri, A magnetic microrobot with in situ force sensing capabilities, *Robotics* 3, (2014) 106–119.

[57] S. A. Morin, R. F. Shepherd, S. W. Kwok, A. A. Stokes, A. Nemiroski, G. M. Whitesides, Camouflage and Display for Soft Machines, *Science* 337 (2012) 828–832.

[58] J. Cui, T. Y. Huang, Z. Luo, P. Testa, H. Gu, X. Z. Chen, B. J. Nelson, L. J. Heyderman, Nanomagnetic encoding of shape-morphing micromachines, *Nature* 575 (2019) 164–168.

[59] S. Li, R. Batra, D. Brown, H. D. Chang, N. Ranganathan, C. Hoberman, D. Rus, H. Lipson, Particle robotics based on statistical mechanics of loosely coupled components, *Nature* 567, (2019) 361–365.

Author contributions

Z.W., H.D. and X.K. conceived the concept. X.K., S.Z., Z.C. and J.J. carried out the experiments and data processing, X.K. and Z.W. set up the theoretical model and drafted the manuscript. Z.W. and H.D. directed the project. All authors participated data analysis and commented on the manuscript.

Declaration of competing interest

The authors declare that they have no competing interests.

Acknowledgments

The materials based on the work partly financially supported by National Key R&D program of China (2017YFB1303100) and National Science Foundation of China (U1613204).

Appendix A. Supplementary data

All data needed to evaluate the conclusions in the paper are present in the paper and/or the Supplementary Materials. Additional data related to this paper may be requested from the authors.

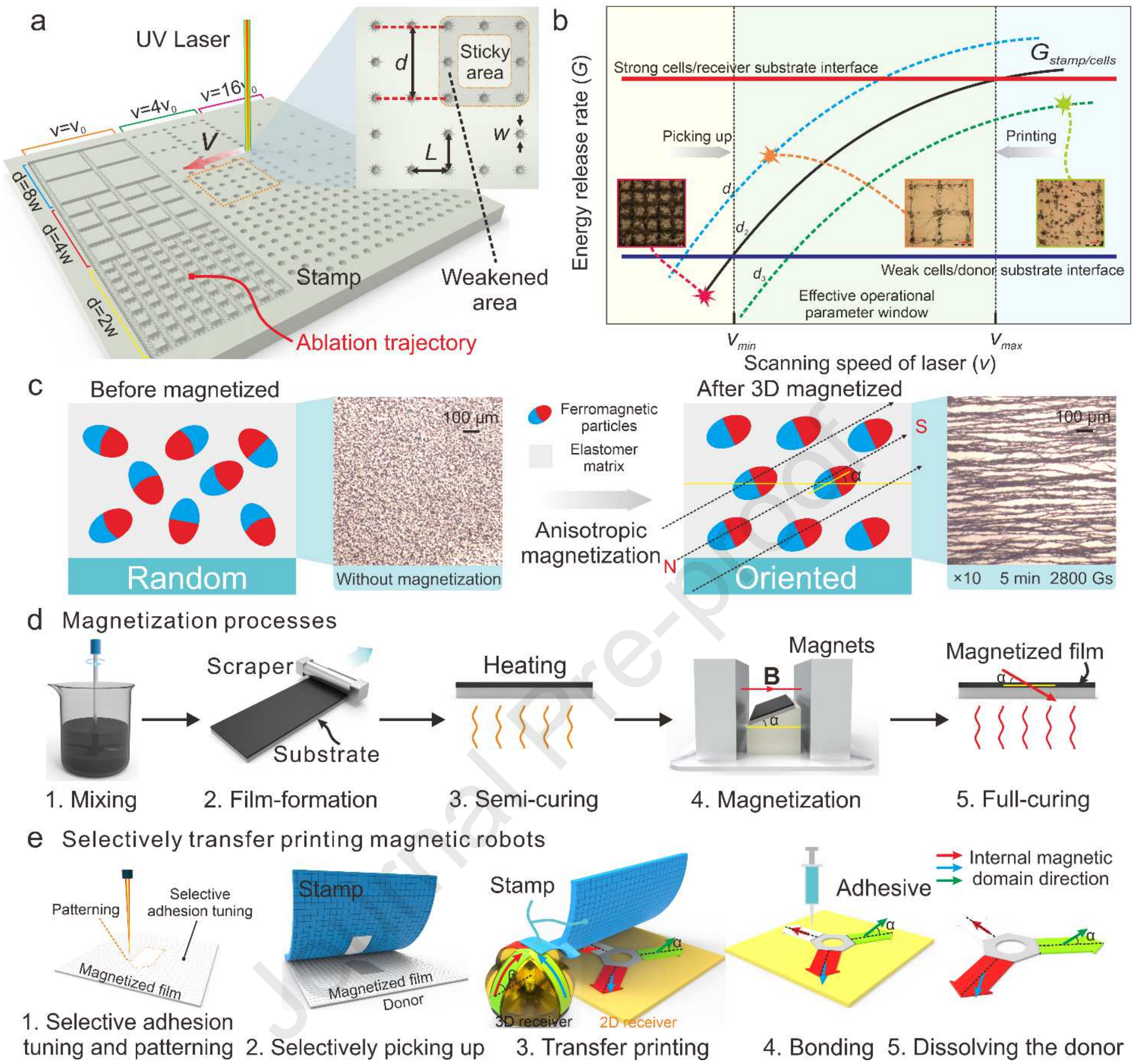

Fig. 1. Soft magnetic robot fabrication by selectively transfer printing. (a) Schematic illustration of typical settings and parameters for surface adhesion tuning by a surface laser scanning. (b) Analytical diagram of critical energy release rates for the stamp/cells interface, cells/donor substrate interface (weak interface) and cells/receiver substrate interface (strong interface). The surface adhesion of stamp or magnetized film can be tuned by laser surface treatment under different scanning speed and scanning distance, which can easily tune the critical energy release rates for the stamp/cells interface to satisfy the transfer printing criteria. (c) Schematic magnetization mechanism. (d) Arbitrarily magnetized film preparation processes. (e) Selectively transfer printing soft magnetic robots on 2/3D soluble receivers.

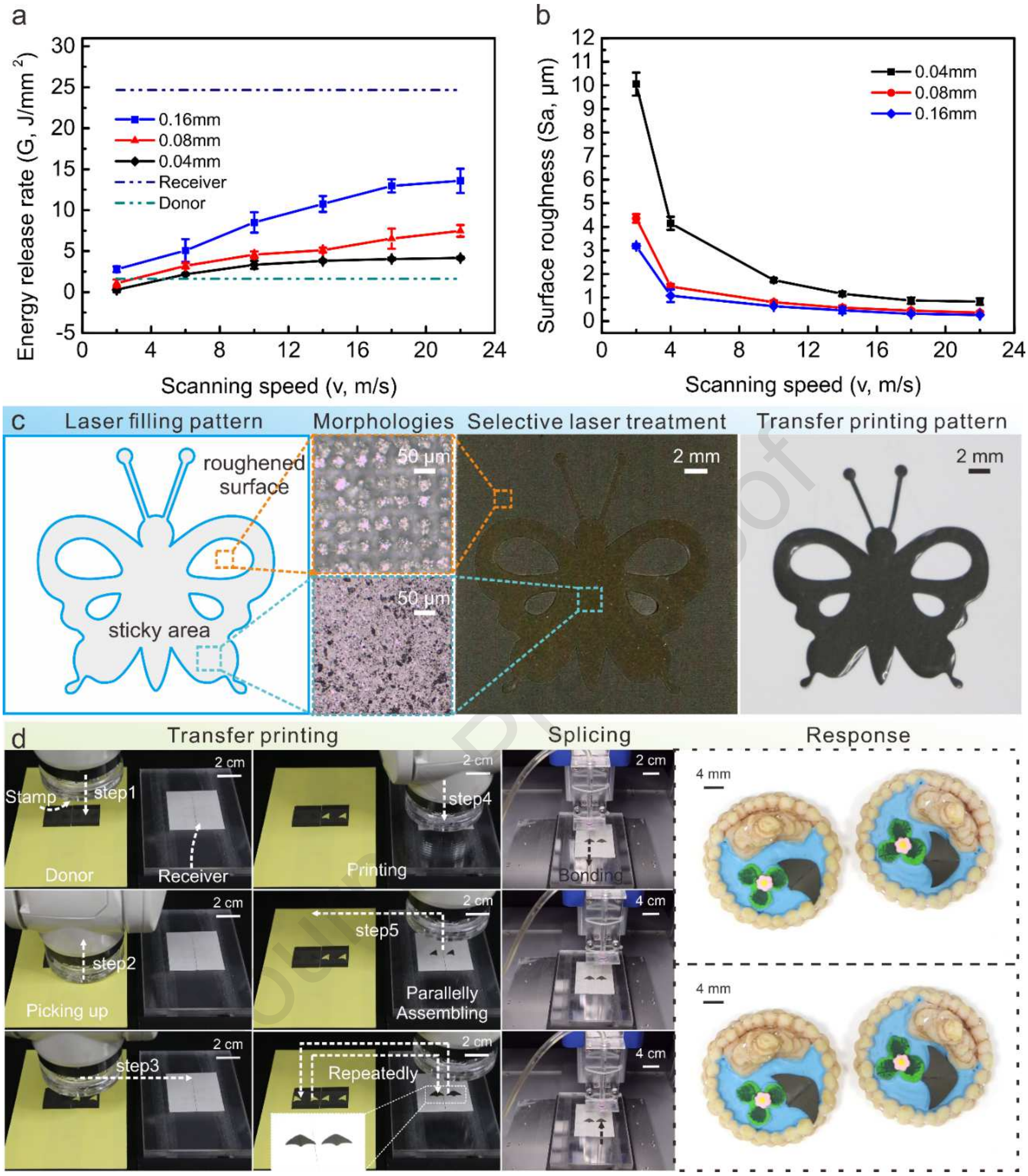

Fig. 2. Surface adhesion tuning and selective adhesive transfer printing. (a) Tuning energy release rate between the cells and stamp by modifying laser parameters (laser scanning speed, *v*, and scanning line spacing, *d*). (b) The surface roughness of laser surface treated stamp cells under various laser operation parameters. (c) Selectively transfer printing of a magnetic butterfly by tunable surface adhesion: selectively setting laser operational parameters on the magnetized film and thus causing different adhesion during transfer printing process. Laser selective treated magnetized film for transfer printing of a butterfly can be obtained leveraging above method. The magnetic butterfly that was selectively transfer printed. (d) Automatically parallelly printing of two magnetic ray robots by an industrial robot and a dispenser system and their response behaviors immersed in the water environment.

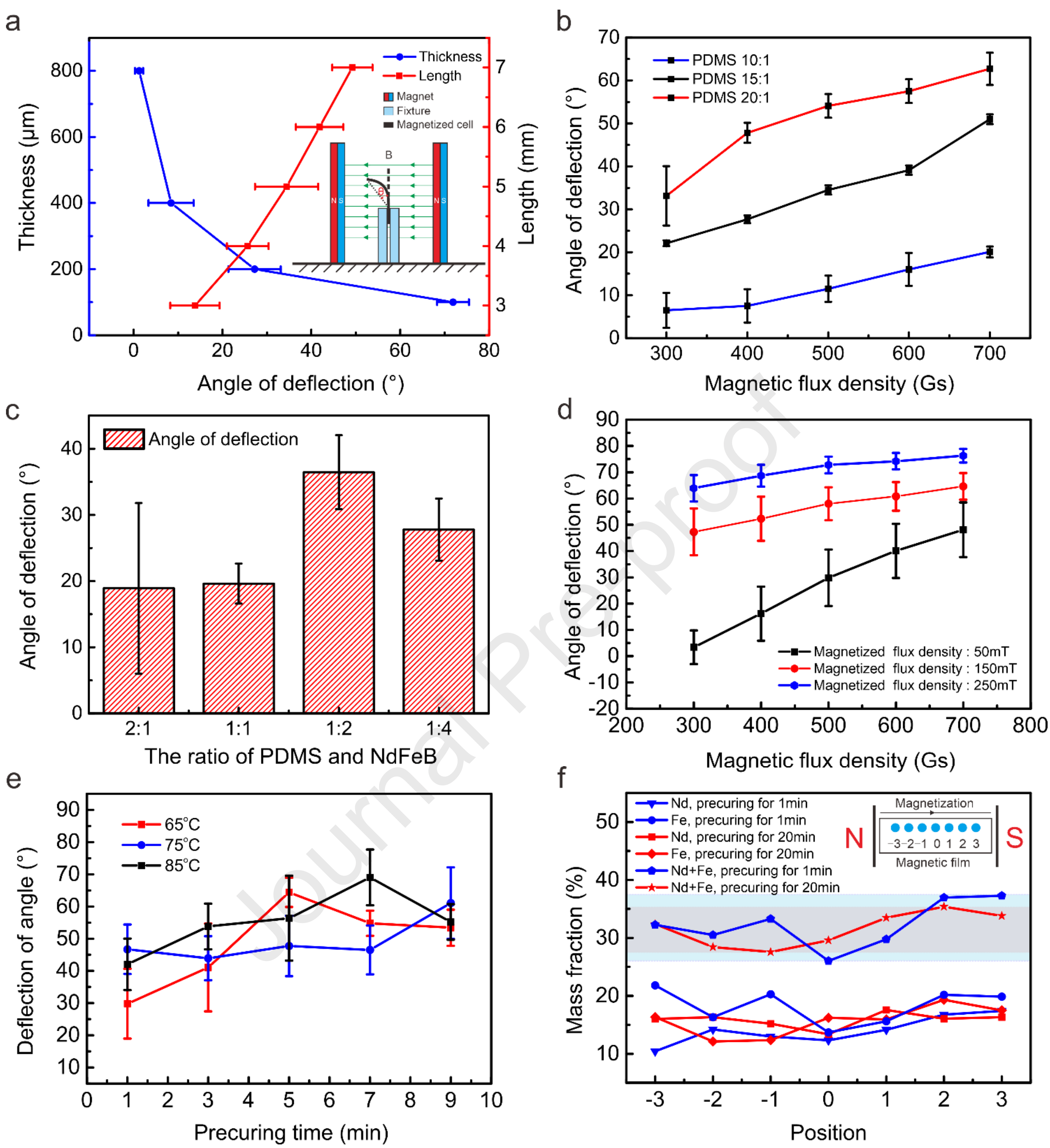

Fig. 3. Characterization of ferromagnetic silicone cells response to magnetic fields under various factors and magnetic particles distribution with different precuring time and temperature. (a) Effects of geometrical parameters of cells on the response characteristics and the setup of test platform for charactering the response characteristics. (b) Effects of different component ratio of PDMS on the response characteristics. (c) Effects of the ratio of PDMS and microparticles of NdFeB on the response characteristics. (d) Effects of the magnetized flux density on the response characteristics. (e) Effects of the precuring time on the response characteristics. (f) Effects of the precuring time on the distribution of the microparticles of NdFeB.

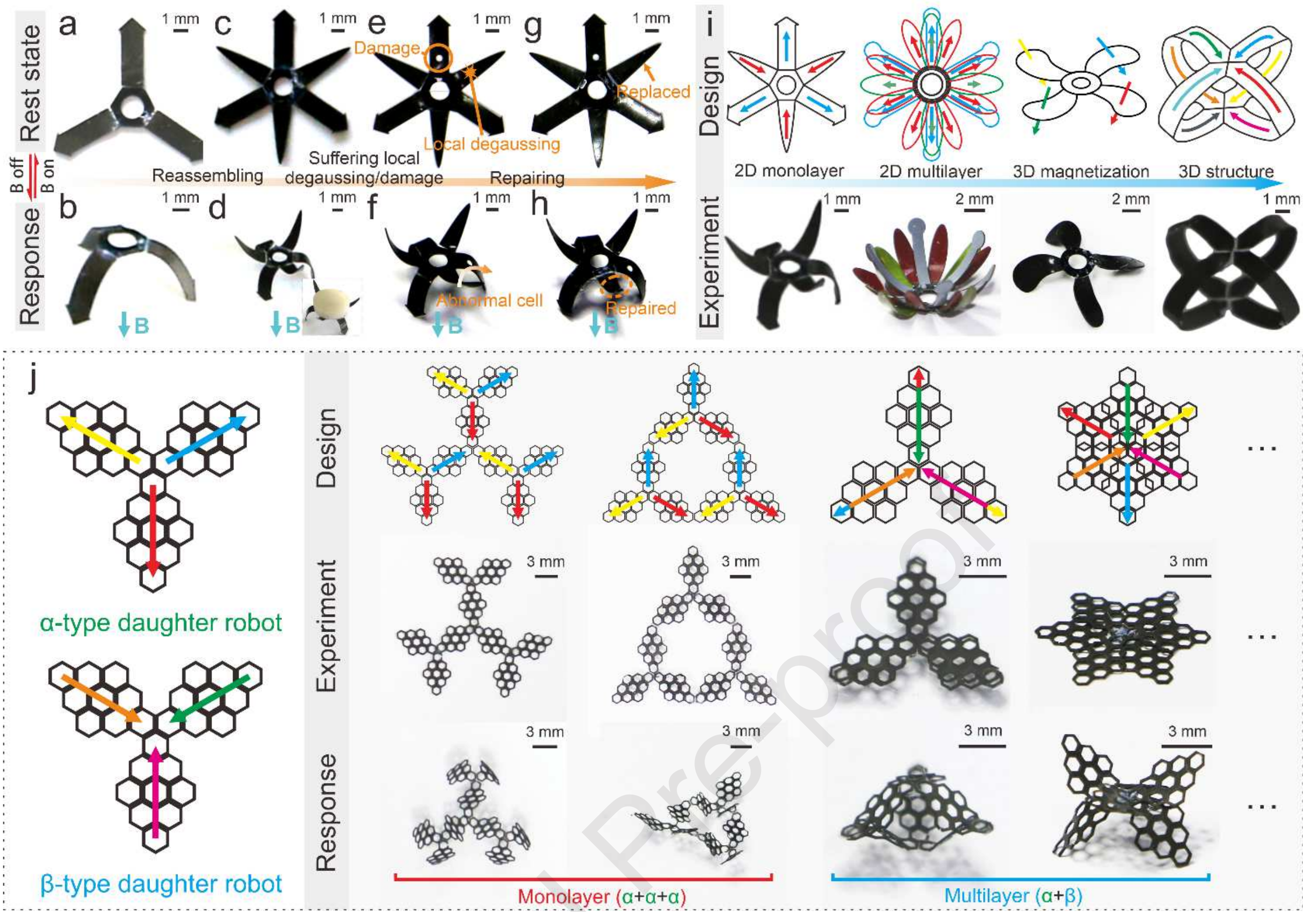

Fig. 4. Configurable modularized magnetic robots: function updating, repairing, transfer printing of various magnetic robots with different magnetic profiles and shapes, recombination of homologous daughter robots. (a-b) A three-legged robot in the rest state and response state, respectively. (c) A weight-lifting robot that is transformed from the three-legged robot by reprinting three arm cells. (d) The weight-lifting robot under the magnetic fields lifts a cargo that is five times weight to itself. (e-f) The weight-lifting robot suffered from local degaussing and local damage. (g-h) The weight-lifting robot was repaired by replaced the abnormal cell. (i) Demonstrations of various magnetic robots with different magnetization profiles and shapes. (j) Reconfiguration of the magnetic robots employing homologous daughter robots with different constraints and corresponding response behaviors in the water environment under the actuation magnetic fields.

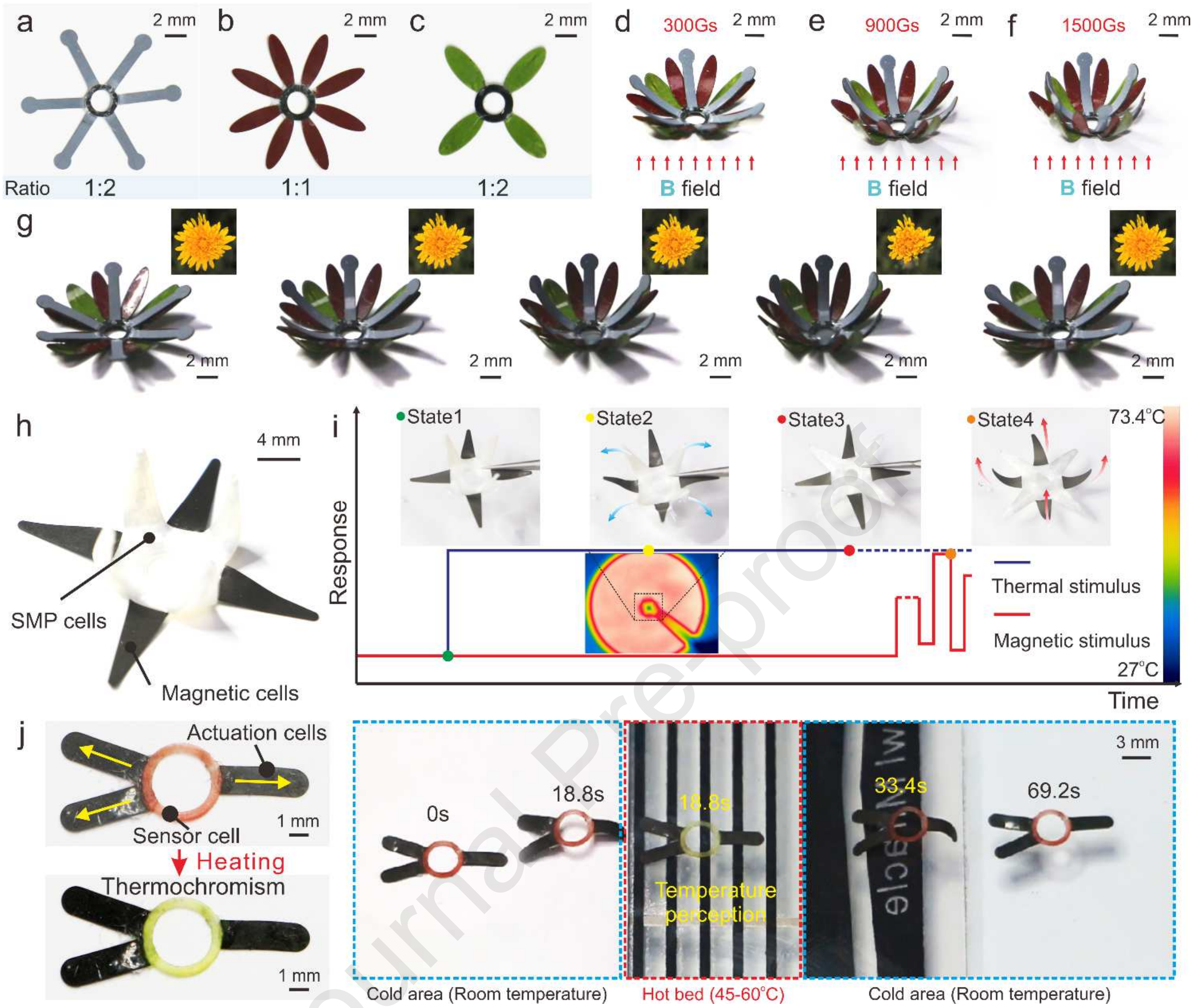

Fig. 5. Heterogeneous integration of different responsive, actuation and functional cells. (a-c) Three kinds of petals with different ferromagnetic particle concentrations and gradient response characteristics. (d-f) Recombinant flower-like structure with gradient responses under a magnetic field of 300Gs, 900Gs and 1500Gs, respectively. (g) Mimicking the blooming process of the dandelion flower. (h) A multi-field actuated robot by heterogeneously integrating SMP cells and magnetic cells together. (i) Sequential actuation in the hot water environment under the thermal stimulus and magnetic stimulus, respectively. (j) Heterogeneous integration of actuation and sensor cells on a three-legged magnetic robot for surficial temperature perception during locomotion.

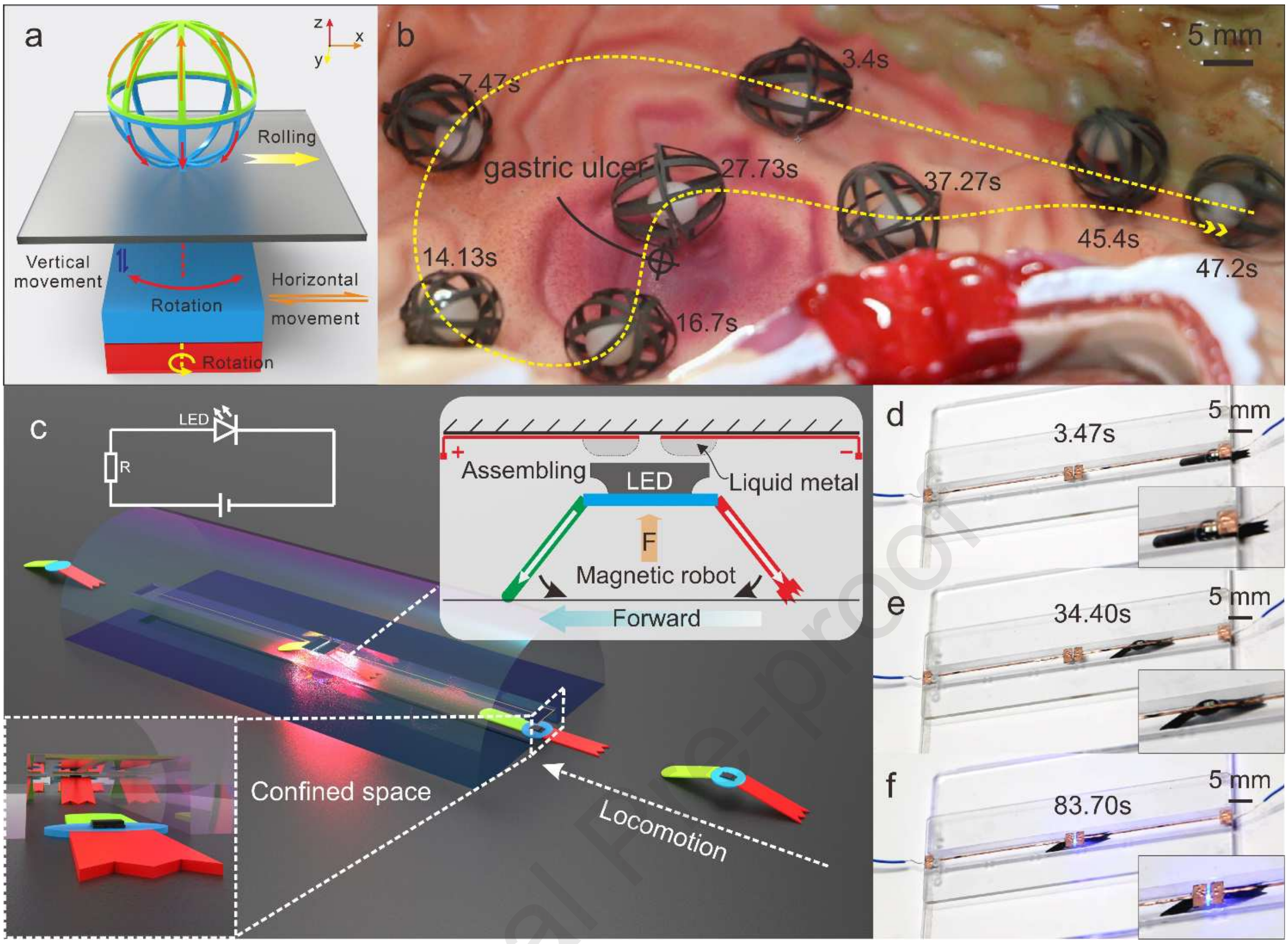

Fig. 6. Application demonstrations of soft magnetic robots. (a) The schematic of the shape and the magnetic domain profiles of the tumbleweed-inspired robot and corresponding actuation setup. (b) A tumbleweed-inspired robot achieved targeted drug delivery in a gastric model filled with water. (c-f) Demonstration of an inchworm-like magnetic robot for an SMD LED delivering and functional circuits assembling in a confined space.

Supplementary Information

Flexible Discretely-Magnetized Configurable Soft Robots via Laser-tuned Selective Transfer Printing of Anisotropic Ferromagnetic Cells

Xingxing Ke [a], Shuo Zhang [a], Zhiping Chai [a], Jiajun Jiang [a], Yi Xu [a], Bo Tao [a], Han Ding [a, **], Zhigang Wu [a, *]

[a] State Key Laboratory of Digital Manufacturing Equipment and Technology, School of Mechanical Science and Engineering, Huazhong University of Science and Technology, Wuhan 430074, China

* Corresponding author, ** Corresponding author.

Email: zgwu@hust.edu.cn (Z.W.); dinghan@hust.edu.cn (H.D.)

The PDF file includes:

Appendix

Figure. S1. Surface three-dimensional contours of the stamp treated by a UV laser under the different parameters respectively.

Figure. S2. The ultra-depth view of diverse surface morphologies by varying laser scanning parameters.

Figure. S3. The actuation platform and the response characteristics platform.

Figure. S4. The relationship among scanning speed, distance of laser and energy release rate.

Figure. S5. FSEM view of the PDMS mixed with magnetized Ferromagnetic particles.

Figure. S6. The EDAX results of different positions of magnetized film.

Figure. S7. Multiple-printing and reconfiguration processes of magnetic robots.

Figure. S8. An inchworm-like magnetic soft robot and its locomotion characteristics under a magnetic field pulse.

Figure. S9. Actuation of wadding gait and its displacement under a periodic external magnetic field.

Figure. S10. The demonstration setup for LED precise assembly by the inchworm-like magnetic robot in a confined space.

Table S1. Capabilities of major methods for fabricating soft magnetic robots.

Other Supplementary Materials for this manuscript includes the following:

Movie S1 (.mp4 format). Assembling an LED in a confined space by an inchworm-like magnetic robot.

Movie S2 (.mp4 format). An ultrathin healed hollow tumbleweed-inspired robot for targeted drug delivery in a model gastric environment.

Movie S3 (.mp4 format). Transfer printing processes of a magnetically-responsive petal.

Movie S4 (.mp4 format). Selectively transfer printing a magnetic butterfly by surface adhesion tuning.

Movie S5 (.mp4 format). Automatically and parallelly printing two magnetic rays.

Movie S6 (.mp4 format). Reconfiguration of daughter robots with different connections and constraints.

Movie S7 (.mp4 format). A magnetically-responsive flower-like structure by combining magnetic stamens, petals and leaves with different concentrations of ferromagnetic particles.

Movie S8 (.mp4 format). Sequential actuation in the hot water environment under the thermal stimulus and magnetic stimulus, respectively.

Movie S9 (.mp4 format). Heterogeneous integration of actuation and sensor cells for temperature perception.

Appendix

Locomotion analysis of inchworm-like magnetic robots and three-legged magnetic robots

An inchworm-like magnetic soft robot was assembled based the above fabrication processes and characterization results. The magnetic robot consisted of two inverse ferromagnetic silicone cells with a different terminal structure that would cause a different frictional force during locomotion (Fig. S8a). With the predesigned discrete distribution of the ferromagnetic domains, the inchworm-like magnetic soft robot can be actuated easily under a pulsed magnetic field perpendicular to the operation plane. As shown in Fig. S8b, by controlling the distance *h* between the planar permanent magnet and operation platform, the magnetic flux density acting on the operation platform changed. Therefore, an approximate periodic magnetic field can be generated by a periodic up-and-down movement of the planar permanent magnet to actuate the magnetic soft robot for a linear motion (Fig. S8c). The planar magnet can move in the horizontal direction synchronously with the magnetic robots in order to maintain a steady vertical magnetic field. Thus, as shown in Fig. S8d, a periodic displacement can be achieved under the trigger of the external magnetic field.

Furthermore, we analyzed the locomotion of the magnetic robot in detail. As shown in Extended Fig. S8e and f, we assume that the frictional force can be divided into static and kinetic friction. When the driving force was lower than the static friction, the feet were anchored; otherwise, movement of the feet occurred resisted by kinetic friction. The locomotion of the inchworm-like magnetic robot is comprised of two movements: front foot movement and rear foot movement. Due to the different tip structures of the feet, the front foot and rear foot can have different maximum static frictional forces (f_{R1} and f_{F2}) and kinetic friction forces (f_{F1} and f_{R2}) on a same actuation platform. F_M represents the force induced by the magnetic field on the ferromagnetic silicone cell.

During the first movement, the front foot slides while the rear foot is anchored on the platform. The state condition is expressed as Equation (S1):

$$f_{R1} > F_M > f_{F1} \tag{S1}$$

During the second movement, the rear foot slides while the front foot is anchored on the platform. The state condition is expressed as Equation (S2):

$$f_{R2} < F_M < f_{F2} \tag{S2}$$

We can further understand the locomotion of the inchworm-like robot and predict the movement by a more elaborate mechanical model based on Newton's second law if we further calculate the magnetic force.

To further verify our understanding on motion modes, a three-legged magnetic robot was designed. As shown in Fig. S9a, the robot moves forward with a swaying gait. This agrees well with our expectations. The periodic actuation magnetic fields can be generated by a pair of permanent magnets oscillating below the actuation platform (Fig. S9b and c), and the angle between the actuation magnet and horizontal plane was defined as ε. The front foot displacement of three-legged robots in five consecutive cycles was recorded (Fig. S9d) and indicates the robust and periodic locomotion.

References

[S1] E. Diller, J. Zhuang, G. Zhan Lum, M. R. Edwards, M. Sitti, Continuously distributed magnetization profile for millimeter-scale elastomeric undulatory swimming, *Appl. Phys. Lett.* 104 (2014) 174101.

[S2] E. Diller, M. Sitti, Three-dimensional programmable assembly by untethered magnetic robotic micro-grippers, *Adv. Funct. Mater.* 24 (2014) 4397–4404.

[S3] J. Zhang, O. Onaizah, K. Middleton, L. You, E. Diller, Reliable Grasping of Three-Dimensional Untethered Mobile Magnetic Microgripper for Autonomous Pick-and-Place, *IEEE Robot. Autom. Lett.* 2 (2017) 835–840.

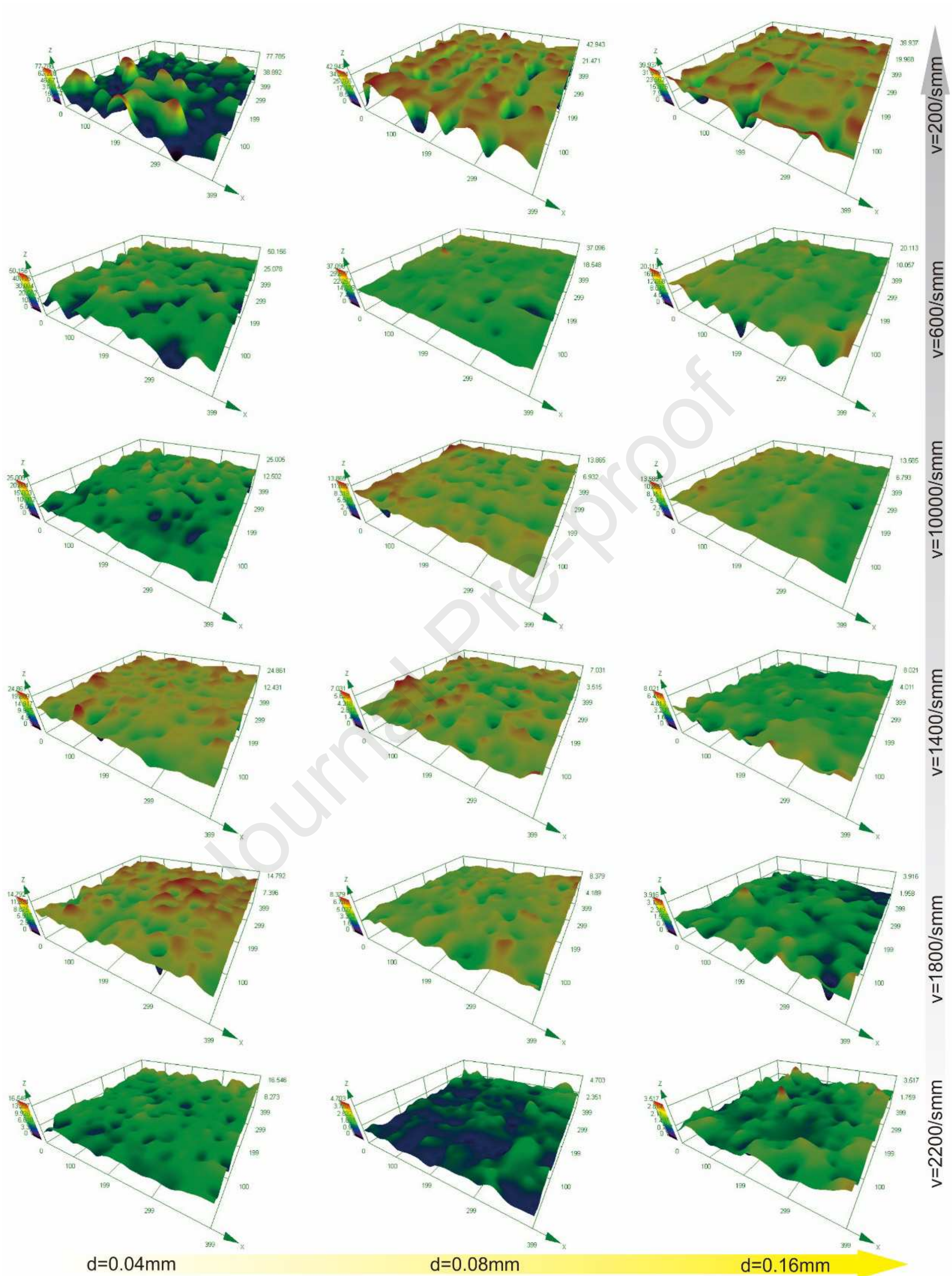

750 **Figure S1.** Surface three-dimensional contours of the stamp treated by a UV laser under the different
751 parameters respectively.

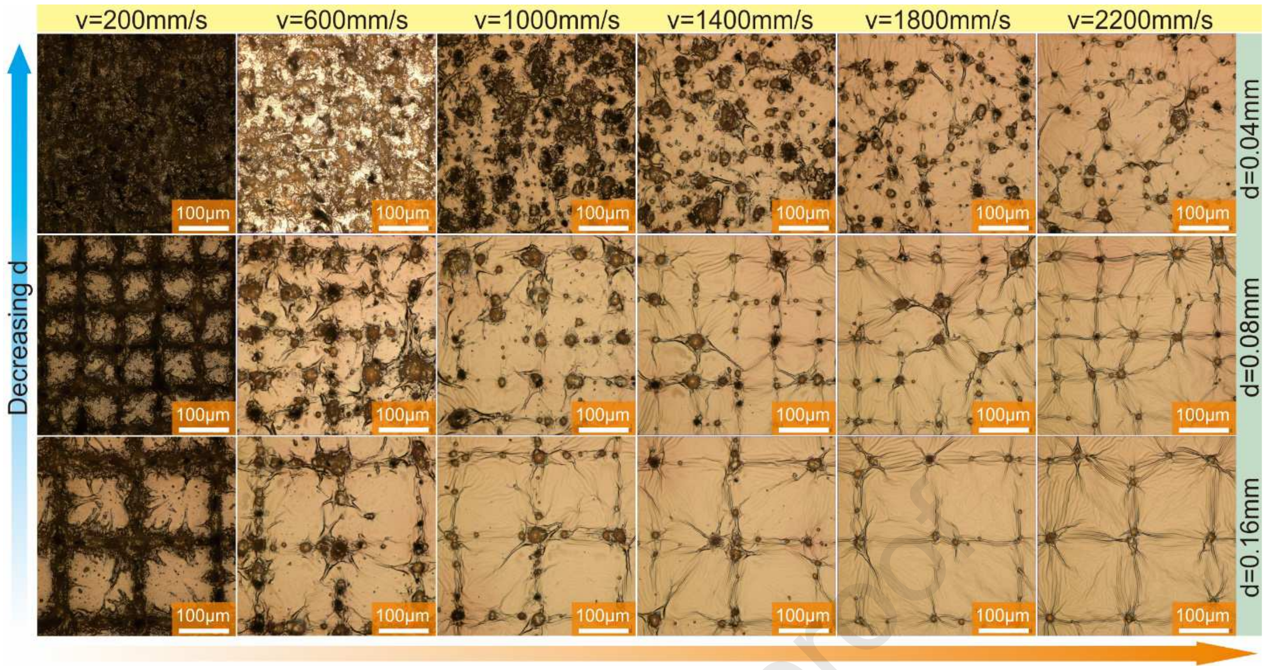

Figure S2. The ultra-depth view of diverse surface morphologies by varying laser scanning parameters.

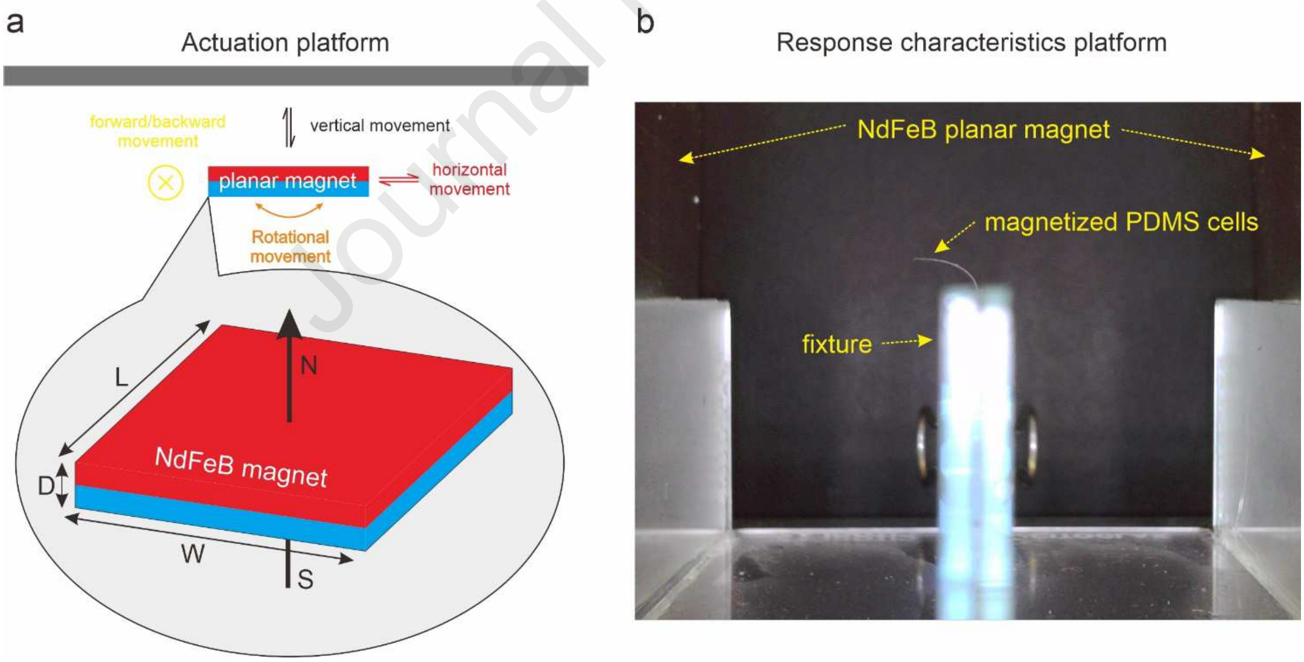

Figure S3. The actuation platform and the response characteristics platform. (a) A planar NdFeB magnet (length of 100 mm, width of 50 mm, thickness of 20 mm, surface flux density of 2500 Gs) was used to create spatially varying magnetic fields for dynamic actuation by combining vertical, horizontal, rotational, forward and backward movements of the magnet. (b) A test platform for quantitatively characterizing the response of the magnetized PDMS cells in specific magnetic fields.

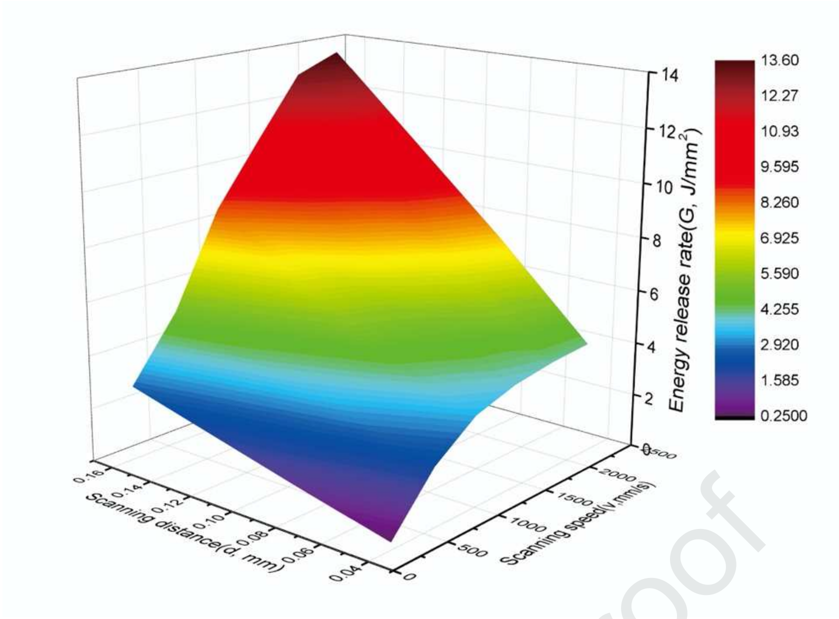

759 **Figure S4.** The relationship among scanning speed, distance of laser and energy release rate.

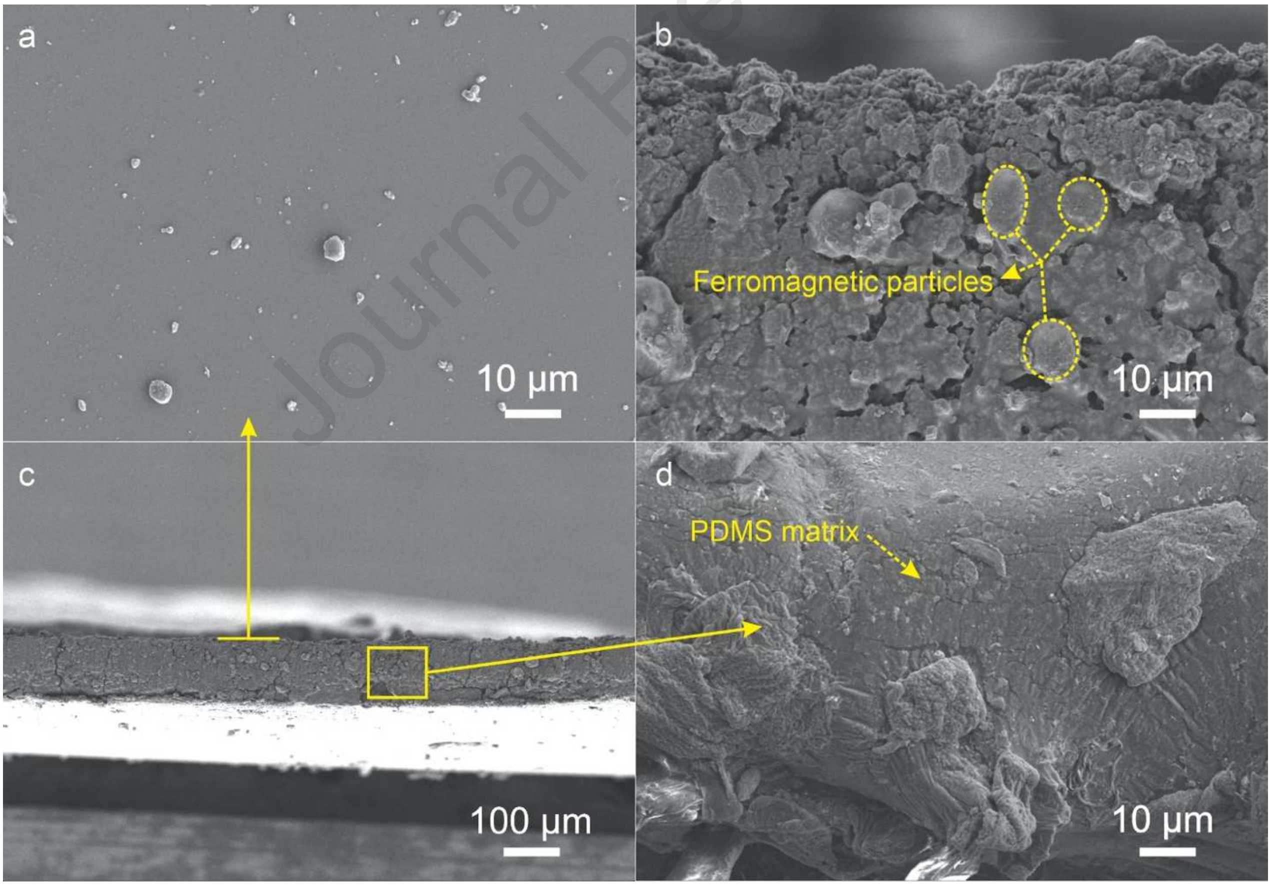

760 **Figure S5.** FSEM view of the PDMS mixed with magnetized Ferromagnetic particles. (a) The
761 surface of the magnetic cells in the top view. (b) The distribution of the ferromagnetic particles in the
762 PDMS matrix in the cross section. (c and d) The distribution of the ferromagnetic particles in the
763 PDMS matrix in longitudinal section.

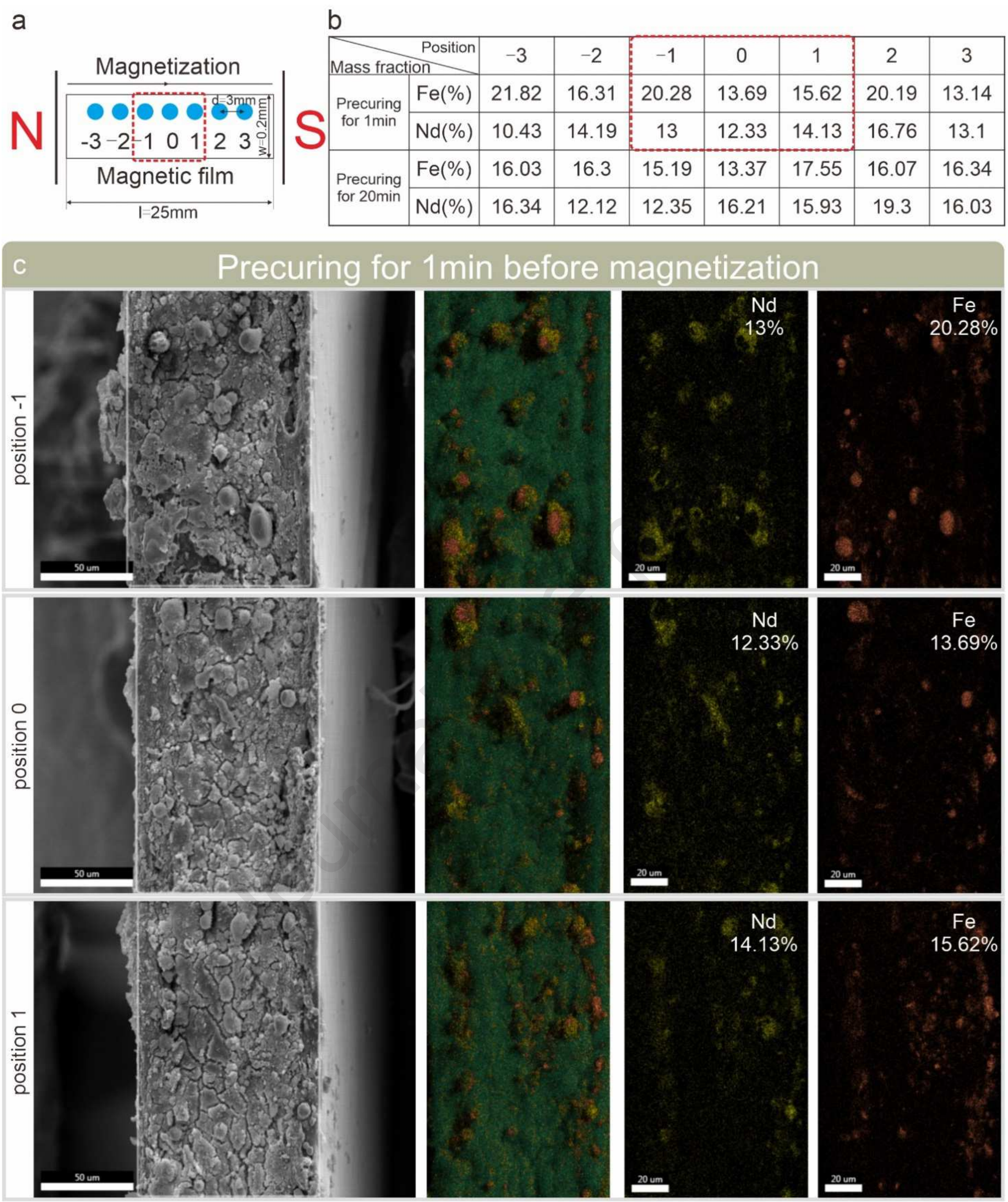

Figure S6. The EDAX results of different positions of magnetized film. (a) Schematic of test position of a magnetized film in cross section direction. (b) Fe and Nd content in various position. (c) The EDAX results in position -1, 0 and 1, respectively.

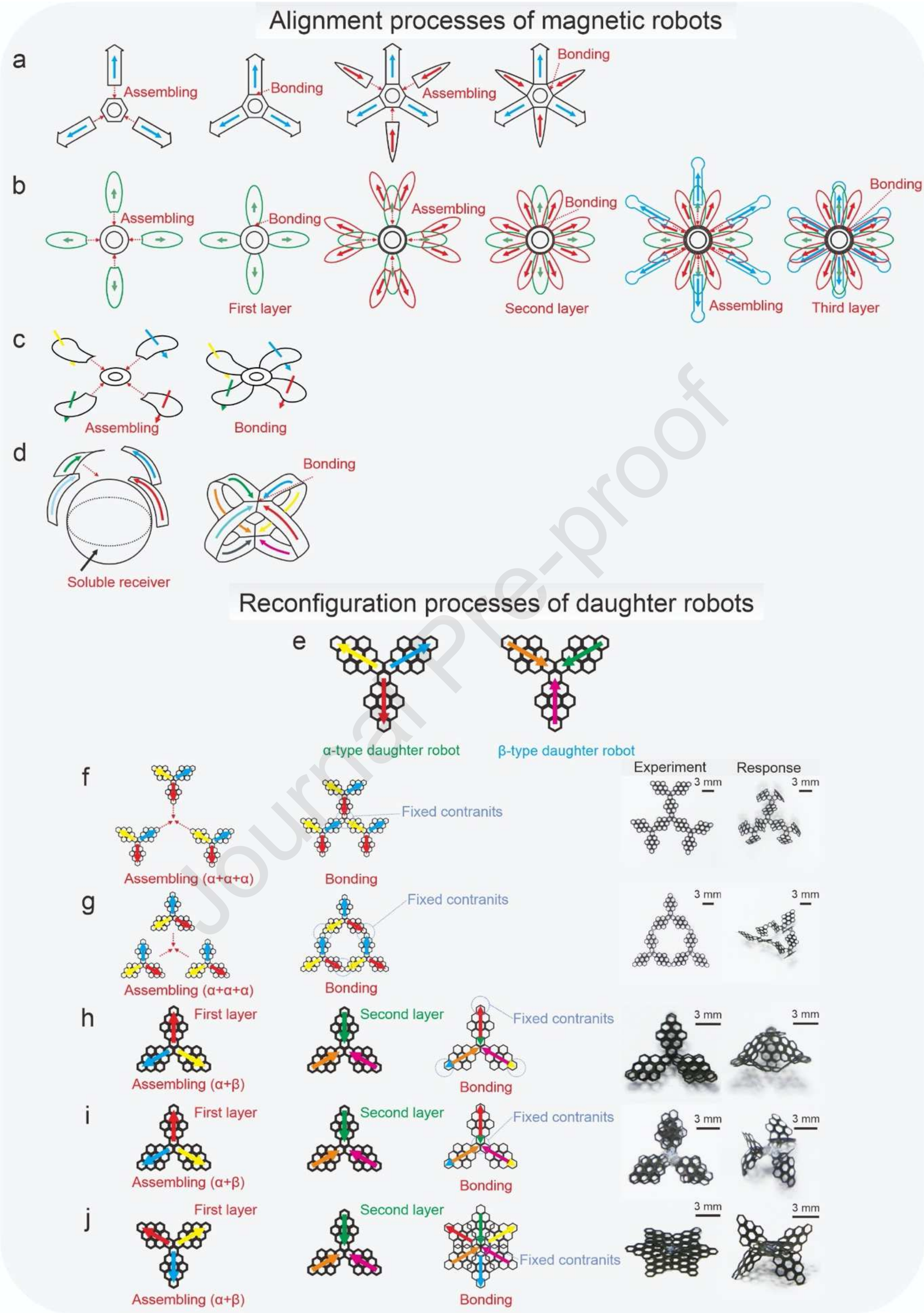

767 **Figure S7.** Multiple-printing and reconfiguration processes of magnetic robots. (a-d) Assembly
768 processes of magnetic robots. (e-f) Reconfiguration processes of daughter robots with different
769 combinations and constraints.

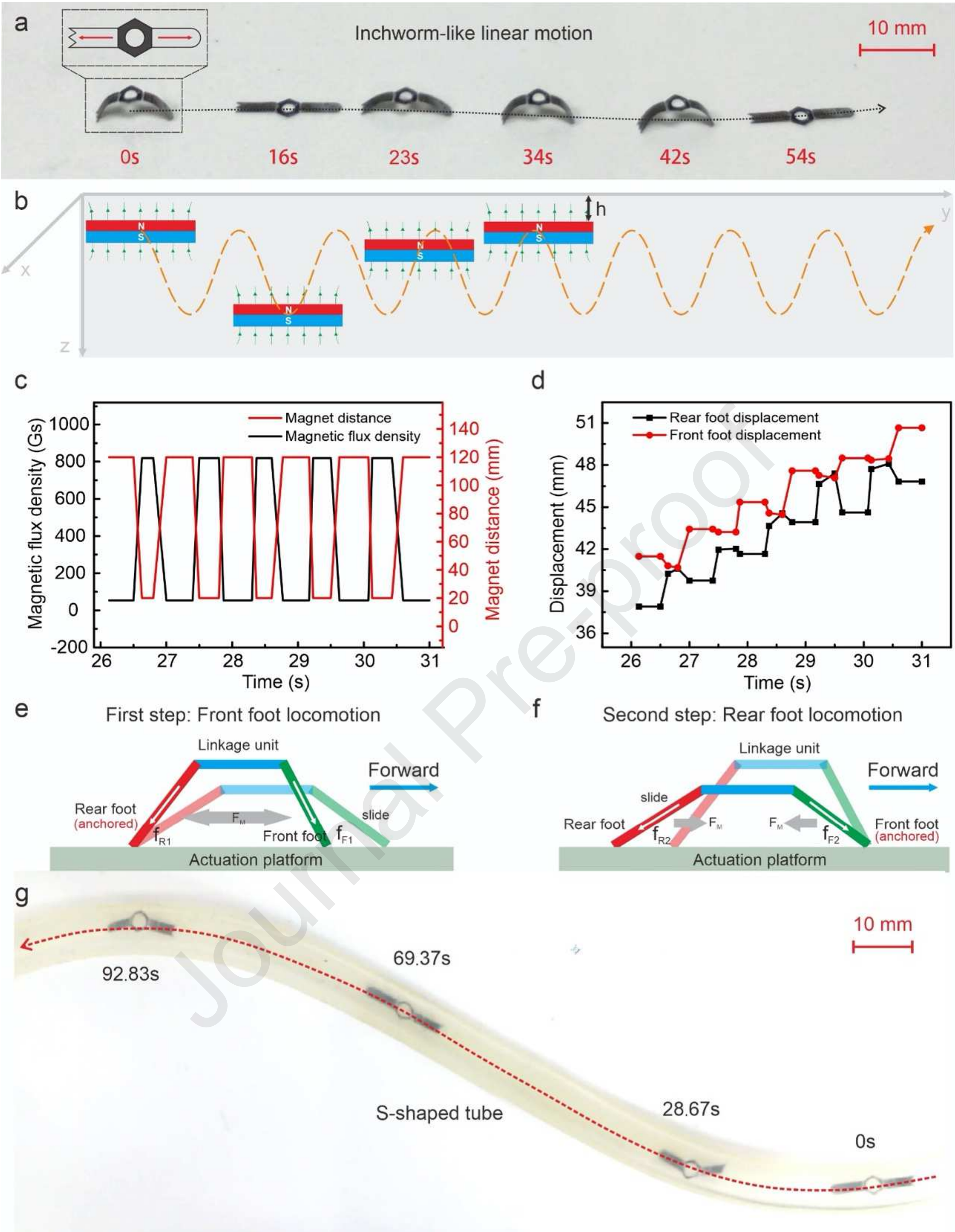

Figure S8. An inchworm-like magnetic soft robot and its locomotion characteristics under a magnetic field pulse. (a) Linear locomotion of an inchworm-like magnetic robot. (b) Motion diagram of planar magnet for actuation of the robot. (c) Actuation magnetic field acting on the platform (x-y plane). (d) The displacement under the magnetic field pulse. (e and f) Two gait states in different steps. f_{R1}, f_{R2}, f_{f1}, f_{f2} represent the static friction of rear foot in step 1, kinetic friction of rear foot in step 2, kinetic friction of front foot in step1, static friction of front foot in step 2, respectively. And the F_M represents the force induced by the magnetic field. (g) An inchworm-like robot walking through the narrow s-shaped tube.

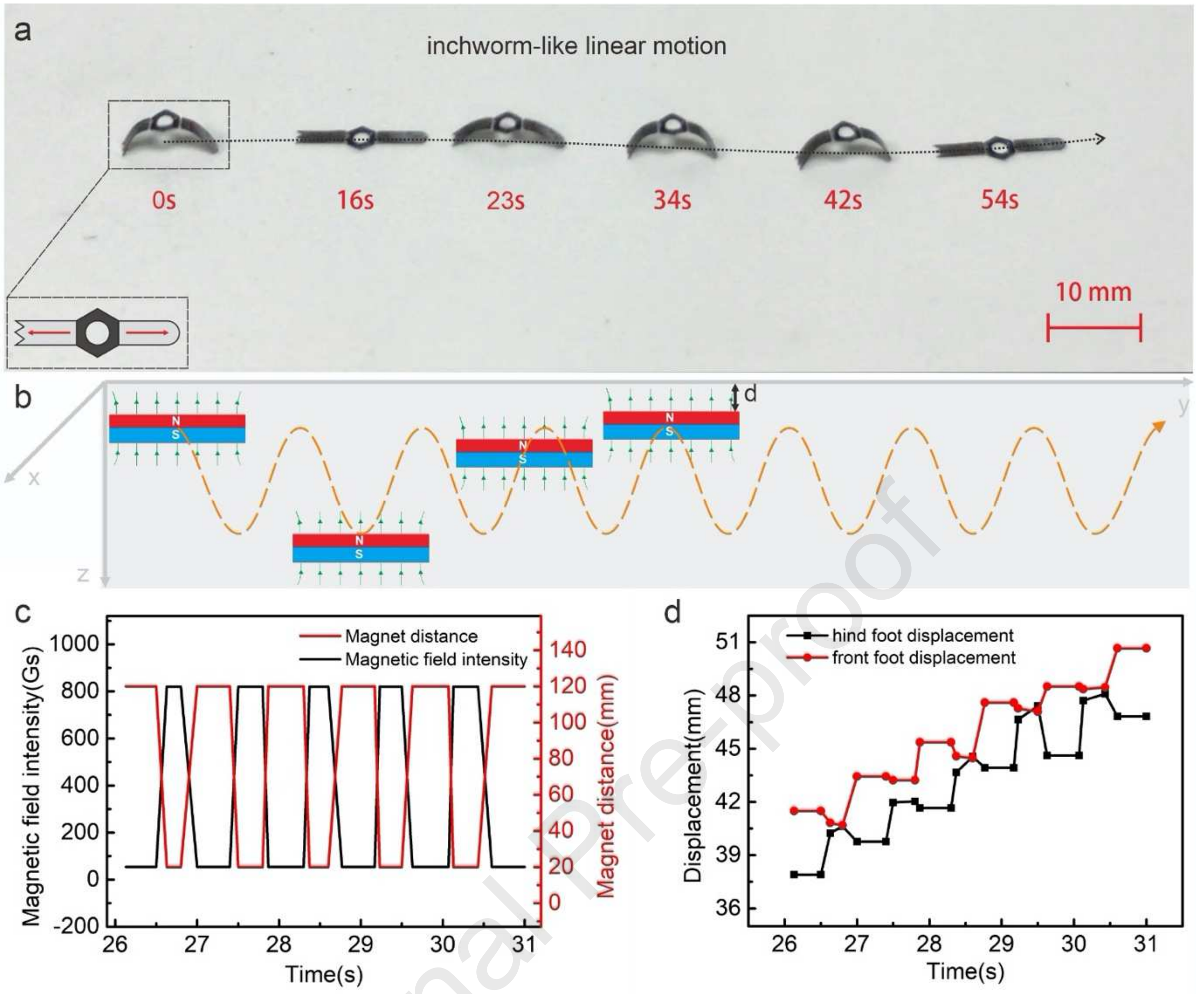

Figure S9. Actuation of wadding gait and its displacement under a periodic external magnetic field. (a) The locomotion of the magnetic robot under wadding gait. (b) Motion diagram of planar magnet for actuation of the robot. (c) The actuation magnetic fields acting on the platform (x-y plane). (d) The displacement under the magnetic field.

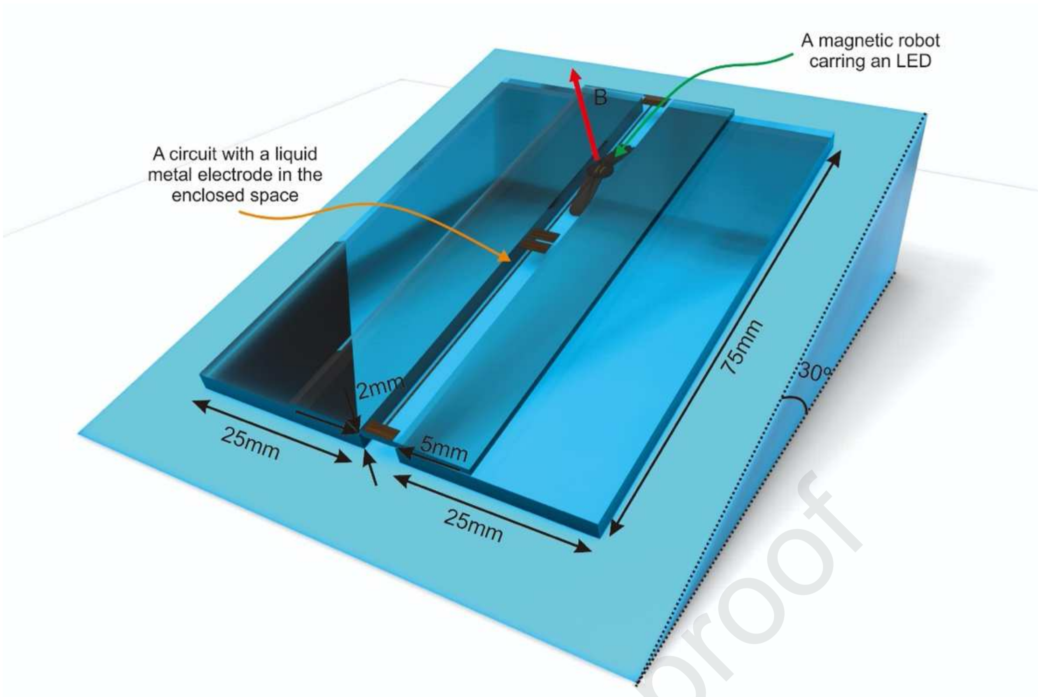

Figure S10. The demonstration setup for LED assembly by the inchworm-like magnetic robot in a confined space.

Table S1. capabilities of major methods for fabricating soft magnetic robots.

Method	Shape of media	States of magnetization	Template or mold required	Heterogeneous integration	Parallel processing capabilities
Template-aided magnetization [23, 30, S1]	2D	Continuum, 3D	Yes	No	Yes
Microassembly of magnetic components [S2, S3]	3D	Discrete, 3D	Yes	No	Yes
Ultraviolet lithography [32]	2D	Discrete, 3D	No	No	Yes
3D printing of ferromagnetic domains [31]	3D	Discrete, 2D	No	No	Yes
This work	3D	Discrete, 3D	No	Yes	Yes

*Shape of media refers to the structure of the composite materials in which the magnetic particles are dispersed. 2D refers to planar structures, whereas 3D refers to solid 3D structures.

*States of magnetization is defined as degrees of freedom related to the orientation of hard magnetic particles or preferred magnetic axes of soft magnetic particles in each area. Discrete: Magnetization in each area is independent of adjacent areas. Continuum: Magnetization in each area cannot have sudden changes with respect to adjacent areas.

Highlights

1) Selective surface adhesion tuning via laser surficial morphology alteration.
2) Selective transfer printing technique leveraging laser selective adhesion tuning
3) A LEGO's strategy to flexibly configure heterogeneous soft magnetic robots.
4) This method is potentially useful for the integration and synergy of multifunctionalities for higher intelligent soft robots

Author contributions

Z.W., H.D. and X.K. conceived the concept. X.K., S.Z., Z.C. and J.J. carried out the experiments and data processing, X.K. and Z.W. set up the theoretical model and drafted the manuscript. Z.W. and H.D. directed the project. All authors participated data analysis and commented on the manuscript.

The author claim that there is no conflict interest is to be claimed.